IOP Publishing J. Phys. Mater. 8 (2025) 022002 https://doi.org/10.1088/2515-7639/adcbd6

Journal of Physics: Materials

TOPICAL REVIEW

Coherent phenomena in exciton–polariton systems

Federico Toffoletti and Elisabetta Collini*

Department of Chemical Sciences, University of Padova, via Marzolo 1, 35131 Padova, Italy
* Author to whom any correspondence should be addressed.

E-mail: elisabetta.collini@unipd.it

Keywords: exciton–polaritons, plexcitons, strong light–matter coupling, ultrafast dynamics, coherence, energy transfer, energy transport

OPEN ACCESS

RECEIVED
24 January 2025

REVISED
25 March 2025

ACCEPTED FOR PUBLICATION
11 April 2025

PUBLISHED
23 April 2025

Original content from this work may be used under the terms of the Creative Commons Attribution 4.0 licence.

Any further distribution of this work must maintain attribution to the author(s) and the title of the work, journal citation and DOI.

Abstract

Exciton–polariton systems, formed through the strong coupling of excitons and photons, provide a unique platform for investigating quantum coherence and collective dynamics in solid-state systems. These hybrid quasiparticles combine photonic and excitonic characteristics, enabling phenomena such as Rabi oscillations, long-distance coherent energy transfer, ballistic energy transport, and Bose–Einstein condensation. Their ability to sustain macroscopic quantum coherence, alongside their sensitivity to environmental and system-engineering factors, highlights their potential for advancing both fundamental quantum science and practical applications, including nanophotonics, energy harvesting, and quantum technologies. This review aims to offer a comprehensive exploration of coherent phenomena in exciton–polariton systems, spanning theoretical foundations, experimental realizations, and applications. Key topics include the dynamics of strong light–matter coupling, the role of vibrational modes and energetic disorder, and the interplay between coherence and dissipation. Advances in ultrafast spectroscopy and quantum electrodynamics models have been pivotal in uncovering polaritonic behavior and optimizing system performance. Despite significant progress, challenges remain in maintaining coherence and addressing the effects of dissipation and disorder. By overcoming these hurdles, exciton–polariton systems promise transformative technological applications and deeper insights into quantum phenomena, positioning them as a cornerstone in the future of quantum science and technology.

List of abbreviations

2DES	Two-dimensional electronic spectroscopy
BEC	Bose–Einstein condensation
BSW	Bloch surface wave
CE	Condition of existence
DBR	Distributed Bragg reflector
DS	Dark state
ER	Exciton reservoir
FRET	Förster resonance energy transfer
FWHM	Full width at half maximum
GS	Ground state
HTC	Holstein–Tavis–Cummings
JC	Jaynes–Cummings
LP	Lower polariton
LSP	Localized surface plasmon
MP	Middle polariton
PSPP	Propagating surface plasmon polariton
QE	Quantum emitter
QEDs	Quantum electrodynamics
QW	Quantum well

© 2025 The Author(s). Published by IOP Publishing Ltd

RWA	Rotating wave approximation
SC	Strong coupling
SLR	surface lattice resonance
TC	Tavis-Cummings
TMD	Transition metal dichalcogenide
UP	Upper polariton
VAS	Vibrational-assisted scattering

1. Introduction

Exciton–polariton systems, formed through the SC of excitons and photons, provide a unique platform for investigating the interplay between light and matter [1–7]. These hybrid quasiparticles, which combine photonic and excitonic characteristics, enable the study of quantum coherence and collective dynamics in solid-state systems. Beyond advancing our understanding of fundamental quantum phenomena, these systems hold promise for applications in quantum computing, photonics, and energy technologies. A defining feature of exciton–polariton systems is their ability to sustain quantum coherence on macroscopic scales. The term 'quantum coherence' generally refers to all oscillating phenomena in a system's observable that exhibit a well-defined phase and frequency, where 'quantum' emphasizes that this coherence originates from the quantum nature of the system. In the SC regime, for example, energy can be exchanged coherently between light and matter, giving rise to phenomena such as BEC [8], superfluidity [9], and coherent energy dynamics [10, 11]. These effects are not only of fundamental interest but also offer avenues for transformative technological applications. Another critical aspect of exciton–polariton systems is their high sensitivity to both the system engineering and environmental factors. These aspects shape coherence and energy transfer processes, introducing new interaction and relaxation pathways. Understanding and controlling these dynamical properties are essential for optimizing system performance and coherence, driving intense scientific interest and research in this field. By exploring exciton–polariton dynamics, this review aims to elucidate the mechanisms underlying coherent behavior and highlight their potential for advancing science and technology. Particular attention will be given to the interplay between light and matter, the factors affecting coherence, and the broader implications of these phenomena.

With this aim, this review is structured to provide a comprehensive exploration of coherent phenomena in exciton–polariton systems, covering their fundamental principles, experimental realizations, and potential applications. In section 2, we begin by introducing the concept of strong light–matter interactions, which form the foundation of polariton physics. This includes a discussion of the basic theoretical frameworks that describe these systems, such as the JC and TC models. These models illustrate how excitonic and photonic states hybridize to form polaritons and how collective effects amplify their unique properties. The role of energetic disorder and vibrational coupling, which significantly influence polaritonic coherence and dynamics, is also analyzed. Building from this theoretical introduction, section 3 transitions to a discussion of the main experimental platforms used to study exciton–polaritons. These include inorganic and organic excitons, microcavities and plasmonic nanosystems. Each platform is explored for its distinct advantages, limitations, and contributions to advancing the study of polaritonic phenomena. This section emphasizes how these systems provide diverse tools for probing the unique interplay of coherence and dissipation in polariton dynamics. Section 4 delves into the dynamics of exciton–polaritons, with a focus on relaxation processes and energy redistribution following excitation. Understanding these mechanisms is critical for interpreting the coherent behavior of polaritons and their interactions with their environment. In section 5.1, we shift to experimental observations of coherent dynamics, such as Rabi oscillations, and their practical implications. This includes an exploration of the unexpected role of vibrational modes in shaping polaritonic behavior. Section 5.2 then presents and discuss some applications derived from the coherent behavior of exciton–polaritons, focusing on polariton-assisted energy transfer, coherent energy transport, and BEC. Finally, in section 6, we conclude with a forward-looking perspective, outlining the remaining challenges in understanding and utilizing polaritonic systems. Potential future research directions are discussed, alongside the exciting opportunities that lie at the intersection of quantum science and real-world applications. Through this structure, the review aims to provide a clear and comprehensive understanding of the rich and dynamic field of exciton–polariton systems, shedding light on both fundamental phenomena and practical innovations.

2. Strong light–matter interaction: theoretical background

The photophysical properties of matter can significantly change under strong light–matter interaction. Specifically, 'Quantum Emitters' (QEs), such as molecules, molecular aggregates, or inorganic excitonic materials, can couple with photons confined within an 'optical cavity.' Once the coupling interactions are

established, various regimes and phenomena can arise depending on the strength of the coupling [1, 3, 7, 12–15]. From a general point of view, in the weak coupling regime, the interaction with light can be viewed as a perturbation of the material system; thus, it facilitates energy exchange between states without significantly altering them. This energy exchange between weakly coupled light and matter states is incoherent and typically enhances the luminescence of the QEs. This phenomenon, known as the Purcell effect, can be attributed to an increased density of states available for the emitted photon [16–19]. Instead, in the SC regime, energy exchange occurs faster than any other decay process, establishing back-and-forth coherent oscillations of the excitation energy. In this situation, light and matter states mix and give rise to two new hybrid states, known as UP and LP, respectively, with an energy separation proportional to the coupling strength. The frequency splitting of these states is referred to as Rabi splitting, denoted as Ω_R , and it corresponds to the frequency of the energy exchange [1, 3, 7, 12–15].

Here, a brief overview of the predominant theoretical descriptions of light–matter interaction in the SC regime is provided. A comprehensive discussion of the theoretical formalisms proposed thus far is beyond the scope of this work; instead, the purpose is to establish a common language essential for understanding the subsequent sections. The section begins with the JC model of a single two-level QE interacting with a single- mode cavity. This is then extended to the Dicke or TC model to accommodate a larger number of QEs coupled to the same cavity, introducing collective phenomena such as the emergence of DSs. Finally, the effects of molecular disorders and vibronic coupling are subsequently introduced.

2.1. JC model

In its simplest form, the effect of SC can be described using a model of two coupled harmonic oscillators that exchange energy. A fully quantum treatment of this phenomenon, involving a single QE interacting with a single-mode cavity, is described by the JC model (figure 1(a)) [7, 14, 20]. In this case, the QE is treated as a two-level system with the ground $|g\rangle$ and excited $|e\rangle$ energy states separated by the transition energy $\hbar\omega_{QE}$, with $\hbar$ being the reduced Planck constant. The Hamiltonian of such an emitter is [7, 14, 20]:

$$\hat{\mathcal{H}}_{QE} = \hbar\omega_{QE}\hat{\sigma}^{\dagger}\hat{\sigma}. \tag{2.1}$$

with $\hat{\sigma} = |g\rangle\langle e|$ and $\hat{\sigma}^{\dagger} = |e\rangle\langle g|$ being the lowering and the raising operator, respectively. On the other hand, the single-mode cavity is described by the standard Hamiltonian:

$$\hat{\mathcal{H}}_{c} = \hbar\omega_{c}\hat{a}^{\dagger}\hat{a} \tag{2.2}$$

with ω_c being the cavity mode frequency, $\hat{a}$ and $\hat{a}^{\dagger}$ the photon annihilation and photon creation operator, respectively. The emitter-cavity interaction is mediated via the electric dipole term:

$$\hat{\mathcal{H}}_{int} = \hat{\boldsymbol{\mu}} \cdot \hat{\boldsymbol{E}}(\boldsymbol{r}_{QE}) \tag{2.3}$$

with $\hat{\boldsymbol{\mu}}$ the QE's dipole moment operator and $\hat{\boldsymbol{E}}$ the electric field operator at the position of the QE ($\boldsymbol{r}_{QE}$). Within the RWA [20, 22] the resulting Hamiltonian in the JC model became [7, 14, 20]:

$$\hat{\mathcal{H}}_{JC} = \hat{\mathcal{H}}_{QE} + \hat{\mathcal{H}}_{c} + \hat{\mathcal{H}}_{int} = \hbar\omega_{QE}\hat{\sigma}^{\dagger}\hat{\sigma} + \hbar\omega_{c}\hat{a}^{\dagger}\hat{a} + \hbar g\left(\hat{\sigma}\hat{a}^{\dagger} + \hat{\sigma}^{\dagger}\hat{a}\right) \tag{2.4}$$

where g is the coupling constant and is defined as:

$$g = -\boldsymbol{\mu}_{eg}\mathcal{E}/\hbar \tag{2.5}$$

with $\boldsymbol{\mu}_{eg}$ the dipole transition moment of the QE, and $\mathcal{E}$ the vacuum electric field. The latter can be expressed through the mode volume V_m as: [22]

$$\mathcal{E} = \sqrt{\hbar\omega/2 \in \in_0 V_m} \tag{2.6}$$

where $\in$ and $\in_0$ are the medium and vacuum permittivity, respectively. From equations (2.5) and (2.6) it is evident that achieving SC requires a large dipole transition moment, and a strong electric field confined in a small mode volume.

In the absence of coupling, the eigenstates of the systems are $\{|g, n\rangle, |e, n\rangle\}$ and represent the direct product of the QE's eigenstates $|g\rangle$, $|e\rangle$ and the cavity Fock states $|n\rangle$, where n indicates the number of photons in the cavity. As a consequence of RWA, the JC Hamiltonian couples only states with the same number of excitations (either QE or photonic excitations), generating new eigenstates from their superposition. Therefore, the global GS is the state with no excitation $|g, 0\rangle$, and it is not affected in the JC picture of interaction. Then, the 'one-particle' excited states rise from the superposition of states with one excitation, which are:

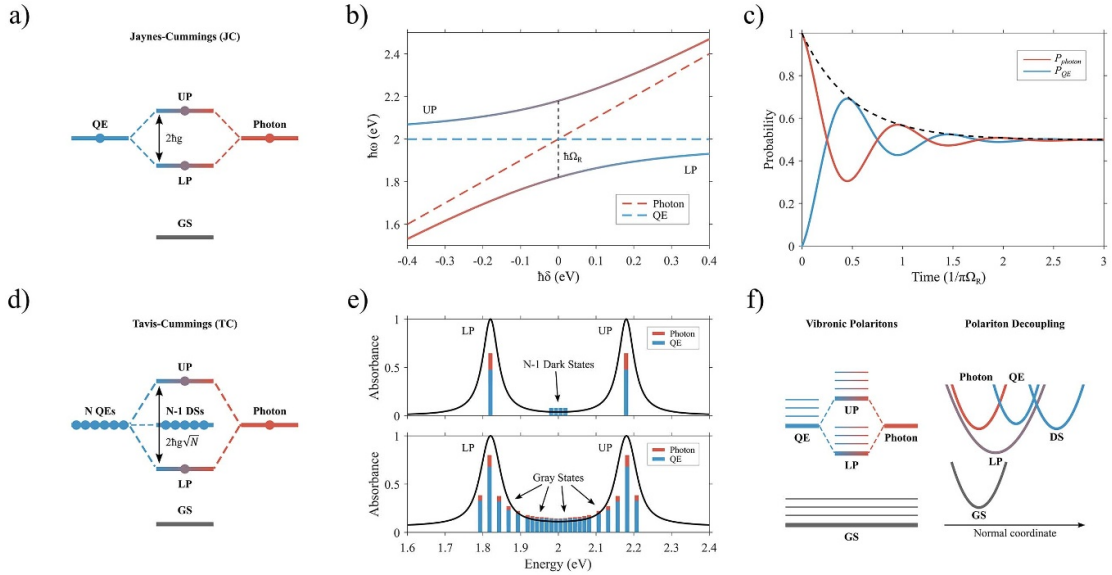

Figure 1. Strong light–matter interaction. (a) The Jaynes–Cummings (JC) model describes the coupling between a single quantum emitter (QE) and a cavity photon, resulting in the formation of upper (UP) and lower polaritons (LP) with an energy split proportional to the coupling strength g. (b) At nonzero detuning, ($\delta = \omega_c - \omega_{QE} \neq 0$), the frequencies of LP and UP exhibit an anticrossing behavior (equation (2.8)); at zero detuning ($\delta = 0$), the LP and UP frequencies are separated by the Rabi frequency Ω_R. (c) Strong coupling is manifested as coherent population oscillation between the QE and cavity, with a frequency equal to the Rabi frequency Ω_R (equation (2.13)). In real systems, these oscillations are damped due to dephasing processes over time. (d) The Tavis–Cummings (TC) model extends the JC framework to include identical QEs (such as in an excitonic state), leading to the formation of $N-1$ dark states (DSs) and increasing the coupling strength by a factor of $\sqrt{N}$. Within this framework, DSs possess zero dipole moment and lack photonic character (equation (2.24)). (e) The addition of disorder transforms the $N-1$ degenerate DSs predicted by the JC model into a broader manifold of 'gray' states which acquire a variable photonic character. Even if highly resilient to disorder, also the LP and UP states are slightly affected by broadening. Reproduced from [5]. CC BY 4.0. (f) When a photon is coupled with a matter system in which the vibrational modes are strongly coupled to the electronic transition (i.e. vibronic coupling), its vibronic structure can be integrated into the polaritonic state landscape, altering energy levels and introducing new properties to the system, as illustrated in the qualitative energy diagram on the left. On the right, the mechanism of polaron decoupling is schematically illustrated. The adiabatic potentials for each state are depicted as a function of a hypothetical normal coordinate. The Rabi splitting magnitude leads to a displacement of the LP potential minimum from that of the QE, effectively reducing the strength of the vibronic coupling. Reprinted from [21], with the permission of AIP Publishing.

(i) the state with the QE in the excited state and no cavity photons: $|e, 0\rangle$
(ii) the state with a single photon and no QE excitation: $|g, 1\rangle$.

Analogously, it is possible to define 'two-particle' and more in general 'n-particle' states. In this review we will focus only on one-particle states, which are the most accessible in conventional experiments. Thus, using $\{|e,0\rangle, |g,1\rangle\}$ as base vectors, the diagonalization of the Hamiltonian (equation (2.4)) leads to the definition of two new eigenstates $|1,-\rangle$ and $|1,+\rangle$, which refer to the LP and UP states, respectively:

$$|1,-\rangle = \alpha|g,1\rangle - \beta|e,0\rangle; \tag{2.7a}$$

$$|1,+\rangle = \beta|g,1\rangle + \alpha|e,0\rangle \tag{2.7b}$$

where α and β are the weights in the linear combination. The resulting eigenfrequencies, displayed in figure 1(b), are:

$$\omega_{\pm} = \frac{\omega_{QE} + \omega_c}{2} \pm \sqrt{\frac{\delta^2}{4} + g^2}; \tag{2.8a}$$

$$\delta = \omega_c - \omega_{QE}; \tag{2.8b}$$

where the detuning δ is defined. In the condition of perfect resonance, i.e. $\delta = 0$, it is verified that:

$$|1, \pm\rangle = \frac{|g,1\rangle \pm |e,0\rangle}{\sqrt{2}}; \tag{2.9a}$$

$$\omega_{\pm} = \frac{\omega_c + \omega_{QE}}{2} \pm g; \tag{2.9b}$$

and the energy difference between the new eigenstates is called Rabi splitting:

$$\Omega_R = 2g. \tag{2.10}$$

In the Schrödinger picture, the temporal evolution is recovered from $\left|\Psi\left(t\right)\right\rangle = e^{-\hat{\mathcal{H}}t/\hbar}\left|\Psi\left(0\right)\right\rangle$. Assuming the cavity to be initially excited and the QE to be in the GS, such as

$$\left|\Psi\left(0\right)\right\rangle = \left|g,1\right\rangle = \frac{\left|1,-\right\rangle + \left|1,+\right\rangle}{\sqrt{2}} \tag{2.11}$$

(note that $\left|\Psi\left(0\right)\right.$ is described as a superposition between the two new eigenstates) after a time t, the state has evolved to [2]:

$$\begin{aligned}\left|\Psi\left(t\right)\right\rangle &= \frac{e^{-i\omega_- t}\left|1,-\right\rangle + e^{-i\omega_+ t}\left|1,+\right\rangle}{\sqrt{2}} \\ &= \cos\left(\Omega_R t/2\right)\left|g,1\right\rangle - \mathrm{i}\ \sin\left(\Omega_R t/2\right)\left|e,0\right\rangle.\end{aligned} \tag{2.12}$$

This allows calculating directly the probability $P_e\left(t\right)$ to find the QE in the excited state $\left|\ e\right\rangle$, and the probability $P_g\left(t\right)$ to find the photon in the cavity:

$$P_e\left(t\right) = \left|\left\langle e,0\right|\left.\Psi\left(t\right)\right\rangle\right|^2 = \frac{1-\cos\left(\Omega_R t\right)}{2}; \tag{2.13a}$$

$$P_g\left(t\right) = \left|\left\langle g,1\right|\left.\Psi\left(t\right)\right\rangle\right|^2 = \frac{1+\cos\left(\Omega_R t\right)}{2};. \tag{2.13b}$$

From these results, illustrated in figure 1(c), it is evident that the cavity and the QE exchange photons at a frequency precisely matching the Rabi splitting frequency. This behavior serves as a key indicator of the coherence in strongly coupled polaritonic states. However, in real systems Rabi oscillations are blurred out by dephasing processes. To account for this, the complex frequencies of the QE, $\omega_{QE} - \mathrm{i}\gamma$, and the cavity, $\omega_c - \mathrm{i}k$, can be phenomenologically introduced. Here γ and k are the QE's and cavity's total dephasing rates, resulting in 2γ and $2k$ FWHM of their extinction spectra. The resulting complex eigenfrequencies in the single excitation subspace are obtained by diagonalizing the following non-Hermitian Hamiltonian [7]:

$$\mathcal{H}_{loss} = \begin{pmatrix} \omega_{QE} - \mathrm{i}\gamma & g \\ g & \omega_c - \mathrm{i}k \end{pmatrix} \tag{2.14}$$

which produces:

$$\omega_{\pm}{}' = \frac{\omega_{QE} + \omega_c}{2} - \frac{\mathrm{i}}{2}\left(\gamma + k\right) \pm \frac{1}{2}\sqrt{4g^2 + \left(\delta - \mathrm{i}\left(\gamma - k\right)\right)^2}. \tag{2.15}$$

From this equation we recalculate the Rabi splitting, i.e. the difference of the two eigenfrequencies in the condition of zero detuning:

$$\Omega_R = \sqrt{4g^2 - \left(\gamma - k\right)^2}. \tag{2.16}$$

This expression indicates that in real systems, Ω_R can be reduced due to dephasing effects. These effects also contribute to the damping of the energy exchange over time, as illustrated in figure 1(c), necessitating the inclusion of an additional exponential decay in equation (2.13).

The CE of the polaritons can be derived from equation (2.16). The Rabi splitting is real-valued only in the condition:

$$2g > \left|\gamma - k\right|. \tag{2.17}$$

However, this condition is necessary but not sufficient to reach SC. The new polaritonic states must also be spectrally resolved from one another. This requirement is satisfied when [2, 7, 15]:

$$\Omega_R > \gamma + k. \tag{2.18}$$

This is known as the SC condition, ensuring the coherent exchange of energy between the QE and the cavity field [2, 7, 15].

2.2. Dicke or TC model

In realistic systems, many QEs are simultaneously coupled to the same cavity. This is characteristic of excitonic states, where multiple QEs are collectively coupled and share the excitation. To describe this scenario, the Hamiltonian must be generalized to account for all possible interactions among N identical QEs and the same cavity. Assuming the RWA, the system is described by the Dicke or TC Hamiltonian (figure 1(d)), which is defined as [23, 24]:

$$\hat{\mathcal{H}}_{\mathrm{TC}} = \hbar\omega_{\mathrm{c}}\hat{a}^{\dagger}\hat{a} + \hbar\sum_{i=1}^{N}\omega_{\mathrm{QE}}\hat{\sigma}_i^{\dagger}\hat{\sigma}_i + \hbar g\sum_{i=1}^{N}\left(\hat{\sigma}_i^{\dagger}\hat{a} + \hat{\sigma}_i\hat{a}^{\dagger}\right);. \tag{2.19}$$

As seen for the JC model, TC model only allows hybrid states in which components share the same number of excitations:

$$\hat{N}_{\mathrm{exc}} = \sum_{i=1}^{N}\hat{\sigma}_i^{\dagger}\hat{\sigma}_i + \hat{a}^{\dagger}\hat{a};. \tag{2.20}$$

For $N_{\mathrm{exc}} = 0$, the global GS of the system is defined as $|g_1, \ldots, g_N, 0\rangle = |G, 0\rangle$, where all QEs are in their GSs and no cavity photons are present. For $N_{\mathrm{exc}} = 1$ there are $N+1$ basis states:

1. The state where all QEs remain in their GSs, and there is a single cavity photon: $|g_1, \ldots, g_N, 1\rangle = |G, 1\rangle$.
2. N states where one QE is excited, and no cavity photons are present: $|g_1, \ldots, e_i, \ldots, g_N, 0\rangle = |e_i, 0\rangle$.

These states form the foundation for describing the hybridization between the QEs and the cavity, leading to the formation of collective polaritonic states. These states are therefore derived through the diagonalization of the TC Hamiltonian:

$$|1, \pm\rangle = \frac{1}{\sqrt{2}}|G, 1\rangle \pm \frac{1}{\sqrt{2N}}\sum_{i=1}^{N}|e_i, 0\rangle \tag{2.21}$$

where we have assumed resonance conditions. The respective eigenfrequencies are:

$$\omega_{\pm} = \frac{\omega_{\mathrm{c}} + \omega_{\mathrm{QE}}}{2} \pm g\sqrt{N}; \tag{2.22}$$

$$\Omega_{\mathrm{R}} = 2g\sqrt{N}. \tag{2.23}$$

Equations (2.22) and (2.23) highlight that the coupling strength is enhanced by a factor of $\sqrt{N}$, indicating that the excitation is collectively shared between the cavity and all the N coupled QEs. Consequently, the overall coupling strength and the Rabi splitting depend strongly on the number of QEs in the system.

Importantly, in addition to the two bright states, the single excitation subspace also gives rise to $N-1$ 'Dark States' (DSs) of the form:

$$|\mathrm{DS}\rangle = \sum_{i=1}^{N} c_i |e_i, 0\rangle \text{ with } \sum_{i=1}^{N} c_i = 0. \tag{2.24}$$

As one can see, these states do not couple to the photonic component, and their energies are identical to the energy of uncoupled QEs. These states are referred to as DSs since the transition dipole moment between the global GS and any of these states is zero. Despite being optically dark, these states play a crucial role in shaping the system's properties and dynamics, serving as reservoirs for excitations and mediating non-radiative pathways. In fact, in exciton–polaritons, DSs are often described in the literature as an 'exciton reservoir' (ER) due to their excitonic nature and their role in relaxation dynamics (see section 4). However, it is preferable to use the term ER more broadly, as in non-ideal systems, this reservoir includes not only DSs but also states from all molecules that do not couple to the photonic state, such as those that are misoriented or located at nodes in the optical field, while still contributing to the photophysics of the system.

2.3. The role of energetic disorder

As anticipated, in most scenarios, the assumption of N identical QEs does not hold due to the presence of inhomogeneous disorder, which is intrinsic to many systems. This disorder arises from variations in the local environment of the QEs, leading to spectral broadening of their transition energies. Such inhomogeneous broadening significantly impacts the polaritonic state landscape, altering both their formation and dynamics.

In fact, while LP and UP are largely resilient to the effects of QEs' disorder due to their delocalized nature imparted by SC [25–27], they could still experience broadening [28–30]. This broadening is limited only when Rabi splitting significantly exceeds inhomogeneous disorder. In contrast, the DSs are hugely affected by the presence of disorder. It is now well-established that disorder induces coupling between the bright and the DSs, transforming the $N-1$ degenerate DSs predicted by the JC model into a broader manifold of 'gray' states that acquire a partial photonic character (figure 1(e)) [28–31]. Additionally, disorder is known to disrupt coherence and induce localization, as described by the Anderson localization model [32]. However, unlike pure excitonic systems, where this model predicts a monotonic increase in localization with increasing disorder until a fully localized regime is reached, the presence of SC with a photon cavity alters this behavior. This was demonstrated by Botzung *et al*, who showed that in a lossless cavity, when the coupling strength exceeds the disorder strength, the DSs with energy close to the photon's energy ($\delta \cong 0$) exhibit a 'semilocalized' nature, even at disorder levels that would otherwise lead to full localization [31]. This semilocalized nature describes a scenario where the DSs remain localized, but this localization is spread across multiple, noncontiguous sites that can be arbitrarily distant from one another. As a result, this phenomenon imparts a delocalized-like character to DSs, which plays a crucial role in facilitating coherent energy transport [31, 33], as also discussed in section 5.2.2. Remarkably, coupling with a cavity not only partially protects the DSs from localization but also enables a regime where disorder enhances delocalization and long-range transport [34–37], aligning with the concept of noise-assisted transport. Specifically, it was demonstrated that after an initial increase in localization, further increasing the disorder leads to a regime where disorder promotes delocalization, eventually reaching a point where delocalization becomes independent of disorder [34–37]. In addition to the delocalized nature, the mixing between DSs and bright states has been demonstrated to increase polaritons lifetime, especially in systems with lossy cavities, thereby enhancing energy transfer efficiency [38].

To summarize, while the extinction spectra of disordered polaritonic systems closely resemble those of an ideal, disorder-free system, their dynamical properties are profoundly altered. This arises from the impact of disorder on the energy levels, their delocalization nature, and the interaction channels between all polaritonic states. Given the complexity and importance of these effects, significant research efforts are focused on understanding and controlling polariton dynamics in disordered environments [28–31, 33–45].

2.4. The role of vibrational modes

A significant complexity arises when considering QEs characterized by vibrational motions. These vibrational modes introduce new degrees of freedom that can act as both an additional source of disorder, leading to all the effects discussed in section 2.3, and as a crucial element of the overall coupling. In fact, while phonons in inorganic systems often act only perturbatively [46], most organic systems are characterized by vibrational modes that are strongly coupled to electronic transitions. In some chromophores, this vibronic coupling can become comparable to the Rabi coupling strength when the system is coupled to a cavity [21, 47–51]. As a result, these vibrational modes do not merely act as a perturbation to the system but instead play a significant role in shaping its energies and dynamics. Therefore, in the interaction picture, the QEs must be treated not as simple two-level systems, but as more complex entities where electronic states are coupled to one or more vibrational modes. The HTC model provides a framework to describe these complex interactions [48, 52, 53]. It extends the traditional TC model by incorporating vibronic couplings, allowing for the exploration of the rich dynamics induced by the interaction of nuclear, electronic, and photonic degrees of freedom. HTC model predicts the emergence of novel polaritonic states, known as vibronic polaritons, i.e. hybrid states where photons are 'dressed' by vibrational quanta (figure 1(f)). Among these, the 'dark vibronic polariton' stands out with unique properties, such as the ability to emit photons with energy lower than that of the originating dark polariton state into the far field through photon leakage [54]. In a recent review, Herrera and Spano rigorously explored these aspects, focusing on the absorption and emission properties, and classified vibronic polariton behavior into three distinct coupling regimes based on the Rabi splitting relative to the parameters of the vibronic coupling [48]. This model has proven to be highly effective in predicting a range of phenomena, including the appearance of vibronic sidebands in absorption and emission spectra, and the polaron decoupling (figure 1(f)). The latter occurs when the Rabi splitting surpasses the vibronic coupling, thereby diminishing the influence of vibronic interactions and protecting the polariton coherence [21, 55, 56]. In this context, achieving a high degree of SC might help maintain coherence by suppressing vibronic interactions.

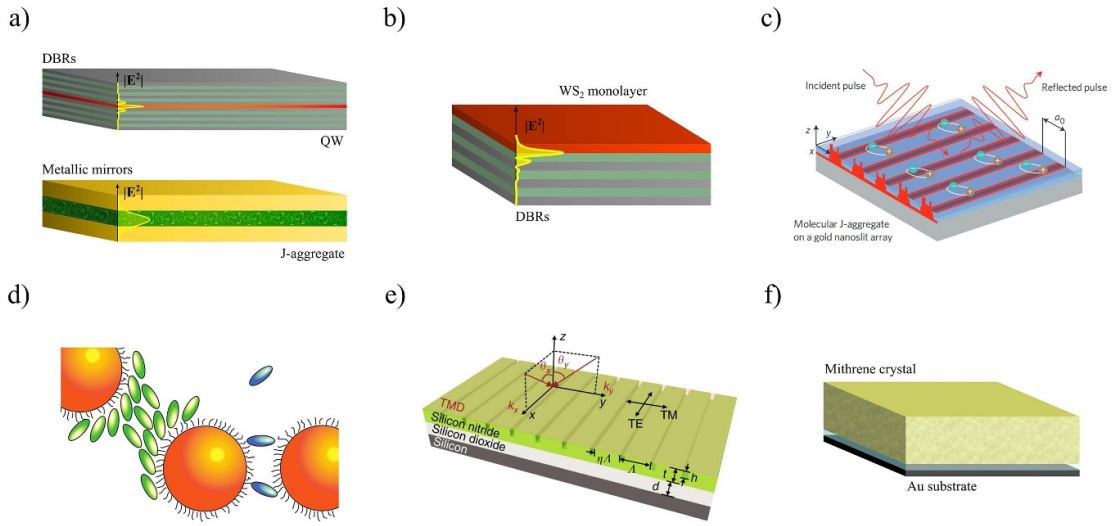

Figure 2. Main classes of exciton–polariton systems. (a) Fabry–Pérot microcavities: The top panel shows a cavity composed of DBRs embedding a monolayer of 2D inorganic semiconductor, such as GaAs QW. The bottom panel illustrates metallic mirrors encapsulating an organic molecular aggregate. (b) BSWs: A dielectric multilayer structure supporting highly confined surface electromagnetic waves coupled to a monolayer of a 2D semiconductor, such as tungsten disulfide (WS_2). (c), (d) Plasmonic cavities: Plasmonic surface resonances enable significant enhancement of the electric field within sub-wavelength dimensions, facilitating strong light–matter coupling with organic excitons and forming hybrid states known as plasmon–exciton polaritons (or plexcitons). These cavities include (c) propagating PSPP cavities, which can be flat or tailored by adding patterns or gratings, with the exciton placed on their surface. Reproduced from [68], with permission from Springer Nature, and (d) LSP cavities, where organic molecules aggregate on the surface of plasmonic nanoparticles, enabling highly confined and enhanced coupling. Reproduced with permission from [69]. © The Royal Society of Chemistry 2021 CC BY 3.0. (e) Photonic crystal cavities: sub-wavelength-thick, one-dimensional photonic crystals hosting a single-layer TMD, enabling strong light–matter coupling. Reproduced from [70]. CC BY 4.0. (f) Self-hybridized exciton–polaritons: Mithrene crystals placed on gold substrates exhibit Rabi splitting in the ultrastrong coupling regime (USC) ($\hbar\Omega_R > 600$ meV), highlighting the advanced capabilities of this compact cavity-free platform [71].

A more thorough discussion on the intricate role of vibronic coupling, both in disrupting and reshaping polariton coherence, potentially paving new pathways for coherence, will be presented in section 5.1.1.

3. Main classes of exciton–polariton systems

In section 2 we discussed the primary theoretical frameworks used to describe light–matter interactions. However, the properties of exciton–polaritons can vary significantly depending on the nature of the excitons (the matter state) and the configuration of the optical cavity (the light state) [1, 7, 57–60]. In this Section, we present a concise, non-exhaustive summary of some of the most common platforms utilized to achieve strong exciton–photon coupling.

Inorganic excitons, such as Wannier–Mott excitons found in materials like GaAs QWs and 2D TMDs, are characterized by weak Coulomb binding energies (5–60 meV) and spatially extended wavefunctions [61]. These properties facilitate strong light–matter coupling, resulting in Rabi splitting values ranging from tens to hundreds of meV, depending on the material and cavity configuration [62]. GaAs QWs often exhibit relatively long polariton lifetimes but require high quality factor cavities. In addition, cryogenic temperatures are typically necessary to minimize phonon scattering and reduce decoherence caused by interaction with the thermal bath [63, 64]. In contrast, TMDs such as MoS_2 and WSe_2 offer higher exciton binding energies, reduced sensitivity to disorder, and the ability to operate at room temperature, making them particularly attractive for practical applications [65, 66]. Inorganic exciton–polaritons dominate in applications where high thermal stability, longer exciton lifetimes, and high-quality microcavity fabrication are needed.

Organic excitons, by contrast, are Frenkel-type, with strong Coulomb binding energies exceeding 1 eV, and are highly localized on molecular scales. Materials such as molecular J-aggregates, organic semiconductors, and hybrid organic-inorganic perovskites enable room-temperature operations, even in cavities with moderate Q-factors (such as plasmonic cavities) [5]. However, polariton lifetimes are typically shorter due to higher excitonic losses, the energetic disorder intrinsic to molecular materials and the vibrational modes. In addition, vibronic coupling can significantly influence the polaritonic landscape and dynamics, introducing complex channels of interaction which often lead to dissipation and decoherence [48]. Organic exciton–polaritons prevail in applications where lightweight, flexible materials, room-temperature operation, and tunable optical properties are prioritized.

The cavity configuration is also crucial in determining polariton properties, such as coupling strength, polariton lifetime, and coherence. Fabry–Pérot microcavities (figure 2(a)) consist of two reflective mirrors separated by a fixed distance; metallic mirrors offer high broadband reflectivity with moderate Q factors (20–100), while high-quality DBRs provide higher reflectivity and Q factors (>1000) at the cost of narrower bandwidth and more complex fabrication. These high-Q factor microcavities support long photon lifetimes and high spatial delocalization of polaritons, making them ideal for applications like polariton condensation and coherent light emission [67]. On the other hand, Fabry–Pérot microcavities based on metallic mirrors exhibit a lower mode volume, which enables higher collective coupling strength, making them ideal platforms for applications such as enhanced intermolecular energy transfer [10].

Another configuration involves BSWs (figure 2(b)). These open cavities, arising from dielectric multilayers, enable high light confinement along the surface of a DBRs, combining low losses and high sensitivity, making them ideal for applications such as sensing and ultra-long energy transport [72–74].

Plasmonic cavities, including PSPPs (figure 2(c)) and LSPs (figure 2(d)), achieve subwavelength confinement and remarkable field enhancement, enabling significant SC even with single molecules or highly disordered excitonic systems [2]. In addition, these systems offer an exceptional design tunability, which can be used to finely tune their optical properties. However, the higher losses inherent to plasmonic systems (low-Q factor of 1–10) reduce polariton lifetimes to few tens of femtoseconds. These systems are also referred to as plasmon–exciton polaritons, or plexcitons.

Recent advances have introduced other innovative systems such as photonic crystal cavities (figure 2(e)), which utilize defect-mode localization and dielectric nanocavities based on Mie resonances. These ultra-compact and practical structures are particularly well-suited for emerging materials like 2D semiconductors and organic thin films, offering low-loss, very high-Q configurations ($\gg 10^3$) that enable robust light–matter interactions and support longer polariton lifetimes [70, 75]. Finally, self-hybridized exciton–polaritons (figure 2(f)) further extend this diversity by exploiting the intrinsic coupling between material excitons and their self-supported photonic modes. This approach creates a compact, cavity-free platform for robust light–matter interactions, and advanced polaritonic applications [71, 76–78].

4. Overview of exciton–polariton dynamics

Building on the understanding of the platforms and mechanisms that enable strong exciton–photon coupling, we now want to give an overview of the main processes contributing to coherent and incoherent exciton–polariton dynamics. The aim of this review is to focus on coherent dynamics, which are dynamics in which a phase relationship between the excited state and the coherent source is maintained over time, enabling a wide range of coherent phenomena and applications [79, 80]. Experimentally, coherent dynamics manifest as oscillatory signals over time (or space) and are typically observed in strongly coupled systems under minimal thermal or environmental perturbations. In contrast, incoherent dynamics arise when the exciton–photon coherence is disrupted by mechanisms that involve interaction with the environment. These include the intrinsic dephasing of the exciton and the cavity, the scattering with phonons [81], the relaxation to ER [82], and fluctuations due to energetic disorder [45]. Therefore, the study of energy relaxation pathways in exciton–polariton systems is vital for understanding their dynamic behaviors and design systems tailored to exhibit desired properties, such as enhanced coherence, improved efficiency, and optimized functionality, ensuring alignment with specific technological objectives. Because of the ultrafast time scale typical of exciton–polariton dynamics, such ultrafast phenomena are difficult to detect and often require the use of advanced ultrafast spectroscopy techniques [38, 41, 55, 68, 83–89].

In figure 3 the main incoherent dynamics that can occur in an exciton–polariton system are shown. One of the main contributors to decoherence in strongly coupled systems is the population transfer from UP to ER [82]. Because of the typically high density of the ER, this transition is very fast, in the order of tens to hundreds of femtoseconds [90–92]. Direct relaxation from the UP to the LP is also possible but less common [87]. Eventually, the UP can relax directly to the GS, a pathway that is favored for UPs with a high photonic character [93, 94] and under high-temperature conditions [95, 96], where the UP is thermally repopulated from the ER (figure 3(a), pathway 1).

From ER, excitation can either relax to the LP or directly to the GS with timescales which are typically longer, reflecting their excitonic nature (figure 3(a), pathways 2–4). Relaxation from ER to the LP occurs primarily through two distinctive mechanisms: radiative pumping and VAS [1, 5, 93, 97–103]. Radiative pumping involves photon emission by an exciton followed by absorption by the LP, and its efficiency depends on the overlap between excitonic emission and polaritonic absorption. In contrast, VAS relies on energy dissipation through Raman-active vibrational modes. While the predominance of one mechanism over the other remains under debate [103], their relative contributions can be deducted based on molecular properties such as the Stokes shift and the spectral overlap between excitonic emission and polaritonic

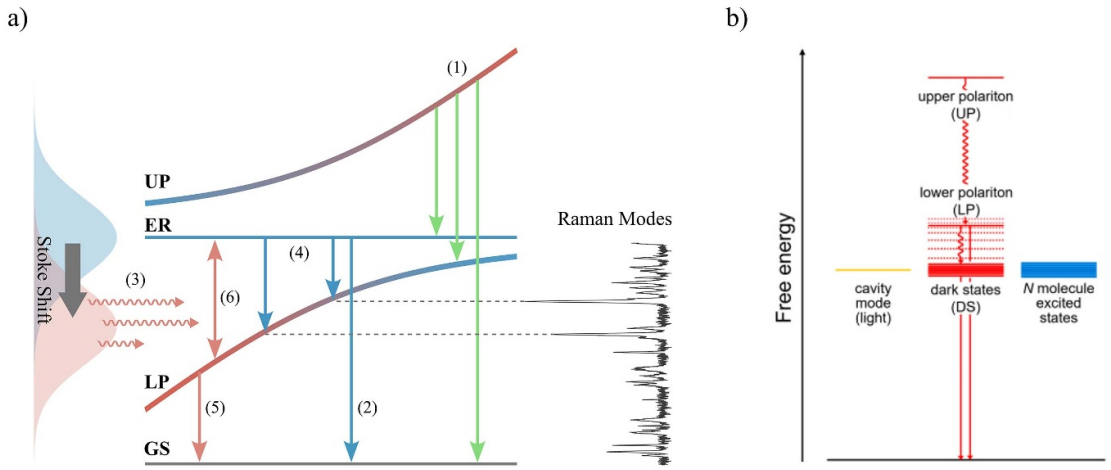

Figure 3. Overview of exciton–polariton dynamics. (a) Incoherent relaxation processes typical of exciton–polariton systems. Reprinted from [97], with the permission of AIP Publishing. (1) The UP can relax to the ER, the LP, or radiatively to the GS (green arrows). From the ER, energy can relax to the GS (2) or transfer to the LP via radiative pumping (3) or VAS (4) (blue arrows). From the LP, the population can relax radiatively to the GS (5) or transfer back to the ER (6) (red arrows). (b) Free energy inversion diagram. Population transfer from the LP to the ER can be promoted by inversion of the free energy landscape due to the high density of states in the ER. Reprinted with permission from [41]. Copyright (2021) American Chemical Society.

absorption [97]. The radiative pumping mechanism dominates in molecules with large Stokes shifts, where high reorganization energy ensures significant overlap. On the other hand, in systems with minimal reorganization energy, such as organic J-aggregates, the minimal overlap between excitonic emission and polaritonic absorption diminishes radiative pumping, making vibrational scattering the primary relaxation pathway. Notably, VAS mechanism requires that the energy gap between the ER and the LP state matches with a vibrational mode. In such cases, excitation of precisely one vibrational quantum above the LP minimum enables efficient single-step relaxation processes [104]. It is noteworthy that, in VAS, phonon scattering is directly involved in the mechanism, while radiative pumping is dictated by light emission and reabsorption, meaning that phonons do not participate directly. However, they play a crucial role by influencing energy reorganization, which subsequently impacts the overlap between the ER's emission and the LP's absorption bands.

The LP typically has a longer lifetime than the UP, often on the picoseconds timescale, and can relax to the GS both radiatively and non-radiatively (figure 3(a), pathway 5). In fact, in exciton–polaritonic systems, emission predominantly originates from the LP [5, 13, 41, 69, 94, 105–107]. Interestingly, the LP lifetime is often observed to exceed the theoretical limits set by cavity and exciton lifetimes [1, 90, 91, 108, 109]. This phenomenon is attributed to the ER, which, as anticipated, can act as an energy reservoir in equilibrium with the LP (figures 3(a), 6). In line with this, Scholes *et al* showed that the entropic gain provided by the density of the DSs' manifold could lead to an inversion of the energy hierarchy, allowing energy to flow from LP states to DSs (figure 3(b)) [110]. This process becomes especially significant in systems with large numbers of QEs, where the entropy plays a dominant role in the energy reorganization. Therefore, to efficiently estimate the intrinsic LP's lifetime, it is crucial to avoid undesired interactions with ER. To address this, some researchers have shown that exciton–polariton dynamics in open cavity systems can be directly measured in the time domain using selective excitation combined with momentum-resolved detection [111]. By utilizing phase-matching conditions, this method reduces the influence of relaxation into the ER, enabling a clearer analysis of LP energy relaxation pathways.

Considering the possibility of relaxation from polaritonic to molecular-localized states, a wide array of novel scenarios can be explored, such as the control of photochemical reactions [112], and singlet fission [21, 113]. This possibility opens pathways for advanced photochemical and photophysical applications, as detailed described by Bhuyan *et al* [1], who highlighted the transformative potential of strong light–matter coupling to manipulate photochemistry and photophysics. Additionally, phenomena that build on the coherent nature of polaritons, such as polariton-assisted energy transfer, coherent propagation of polaritons, and polariton condensation, will be discussed in sections 5.2.1, 5.2.2, and 5.2.3, respectively.

Although the processes described in this overview apply to the majority of exciton–polariton systems, it is important to emphasize that dynamics can vary significantly across different systems, particularly in the case of plasmonic cavities characterized by very high losses. In fact, unlike low-loss cavities, which support well-defined eigenmodes and can be described using discrete sets of harmonic oscillators, high-loss cavities

are governed by complex-valued eigenmodes that can no longer be treated as a perturbation of real valued eigenmodes. This makes the traditional theoretical framework for light–matter interaction described in section 2 inadequate for capturing their full complexity, necessitating the use of more sophisticated QEDs models [1, 114]. Therefore, some authors advise caution when interpreting results or extrapolating general principles from low-loss systems to plasmonic cavities [115]. Additionally, plasmonic systems are strongly influenced by non-radiative processes such as electron–electron scattering which occurs on ultrafast timescales (100–400 fs) and introduce additional decay channels [85, 116]. For this reason, other authors suggest that, following this relaxation, the dynamics in these systems should be described in terms of hot electron distributions rather than using the traditional framework of LP and UP branches [85, 116].

5. Experimental detection of coherent dynamics and applications

5.1. Rabi oscillations

As anticipated in section 2, SC occurs when the energy exchange between light and matter states is rapid enough to permit coherent back-and-forth transfer prior to dissipation. This indicates that energy is coherently shared between light and matter states, and the frequency of this process, known as the Rabi frequency, quantifies the strength of the coupling. Under these conditions, energy becomes delocalized across light and matter states. An unequivocal experimental hallmark of SC is the observation of Rabi oscillations in the populations of the UP and LP states. These oscillations arise from the coherent superposition of the two polaritonic states, confirming the formation of hybrid light–matter states. However, the observable coherence in these systems is often short-lived due to ultrafast dephasing processes. These dephasing processes, depending on the system, can range from a few tens of femtoseconds, typical of plasmonic cavities and organic excitons [68, 92], to a few picoseconds, achievable in high-quality Fabry–Pérot cavities and inorganic semiconductors at cryogenic temperatures [117, 118]. This short coherence duration poses significant challenges for detecting and leveraging these oscillations in practical quantum technologies [45]. Efforts to extend and tune coherence times are focused on optimizing cavity designs [119, 120], tailoring the excitonic environment [45, 82, 121, 122], decoupling polaritons from the thermal bath [21, 55, 56], and tuning the excitation condition [123–125].

Due to these challenges, the Rabi oscillations were observed for the first time by Norris *et al* only in 1994 in high quality planar microcavities embedding inorganic QWs and operating at cryogenic temperatures. Using femtosecond laser pulses, they excited a coherent superposition of polaritonic states producing emission beats with a 600 fs period corresponding to Rabi splitting. This splitting, derived from the energy difference between polariton branches in the reflectivity spectrum, confirmed the system's operation in the SC regime [118]. One decade later, Dominici *et al* expanded this understanding by demonstrating ultrafast control of exciton–polariton Rabi oscillations in a similar semiconductor microcavity system [117]. Utilizing femtosecond spectroscopy, they directly observed and manipulated Rabi oscillations in exciton–polariton systems, which persisted for up to 12 cycles over approximately 10 ps before dephasing occurred.

In contrast, the first direct observation of Rabi oscillations in plasmonic cavities was achieved by Vasa *et al* using femtosecond coherent spectroscopy in 2013 [68]. In their groundbreaking study, J-aggregates of cyanine dyes were deposited onto gold nanoslit array (figure 2(c)), creating a hybrid system where excitonic transitions are strongly coupled with the PSPPs. This coupling led to the formation of hybridized polaritonic states, with a pronounced normal mode splitting indicative of SC, as illustrated in figure 4(a) (top). Using angle-resolved pump-probe spectroscopy, temporal oscillations corresponding to the coherent energy exchange between the LP and UP were observed (figure 4(a), bottom). These oscillations, with a period of around 30 fs, persisted for approximately 50 fs, reflecting the ultrafast nature of these coherent dynamics. Furthermore, the authors demonstrated how it is possible to manipulate these Rabi oscillations by controlling the exciton density on a 10 fs timescale. Despite the SC involving only a small fraction of excitons located near the plasmonic nanostructures, the study demonstrated that femtosecond spectroscopy could capture these fleeting oscillations, providing insights into their underlying physics and suggesting strategies for extending coherence times.

In another significant contribution, coherent Rabi oscillations were detected in colloidal solutions of plexcitonic nanohybrids using 2DES [84]. These nanohybrids comprised gold nanourchins (plasmonic nanoparticles) functionalized with cyanine dye J-aggregates. The 2DES technique revealed diagonal and cross peaks in the spectral maps (figure 4(b), top), directly linked to the hybridized upper and lower plexcitonic states. Oscillatory signals persisted on ultrafast timescales, demonstrating coherent coupling between plasmonic and excitonic modes even in disordered, solution-phase systems and at room temperature. However, the measured dephasing time of these coherent oscillations, approximately 16 fs (figure 4(b), bottom), highlights the challenges associated with the highly lossy nature of plasmonic systems, as discussed in section 4.

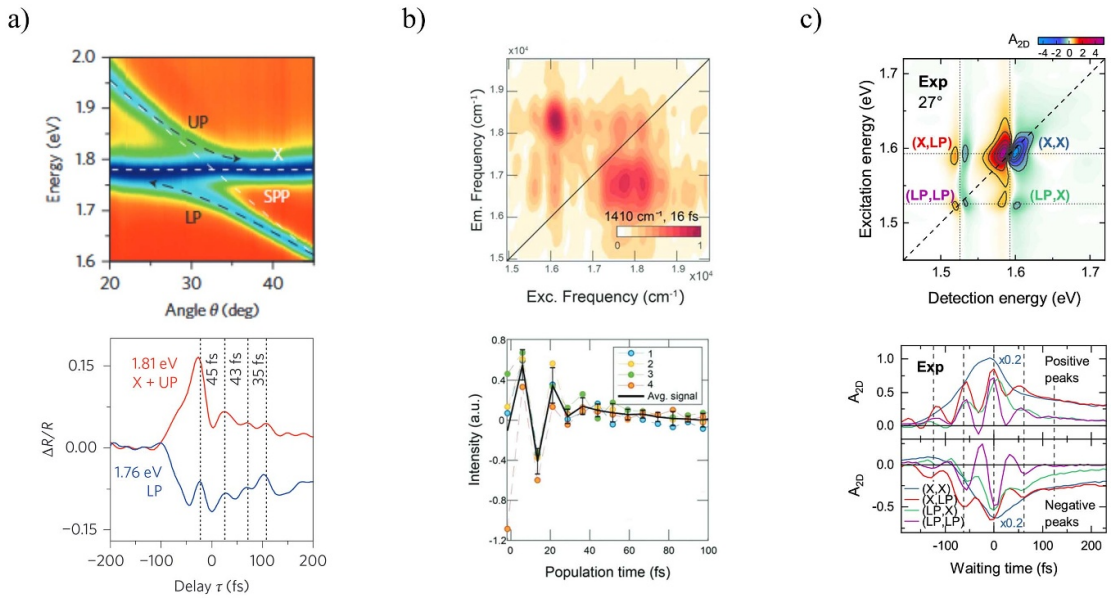

Figure 4. Rabi oscillations. (a) Upper panel: The anticrossing behavior between the UP and LP revealed through angle-dependent reflectivity confirms the SC regime between plasmon and exciton, with a Ω_R of approximately 110 meV. Lower panel: Temporal dynamics of the transient reflectivity at energies near the overlapping between UP and bare J-aggregate resonances (1.81 eV, red curve) and LP (1.76 eV, blue curve). The oscillatory behavior, with periodicities corresponding to the Rabi oscillations, is shown as a function of pump-probe delay (τ). Reproduced from [68], with permission from Springer Nature. (b) Upper panel: The spectral distribution of the oscillating dynamics (Coherent Associated Spectrum) observed in 2DES experiments proves the coherent exchange of energy between lower and upper plexciton states ($\Omega_R \approx 1400\ cm^{-1}$) in colloidal plexcitonic nanohybrids. Lower panel: signal decays (intensity vs time plot) at relevant coordinates. Coherent beatings are reproducibly found with a dephasing time of about 16 fs. Reproduced with permission from [84]. © 2023 The Authors. Advanced Optical Materials published by Wiley-VCH GmbH CC BY 4.0. (c) Upper panel: the experimental 2DES map collected at $t = 0$ revealed coupling interaction between the LP and the weakly coupled exciton X in a system obtained J-aggregate excitons collectively coupled to a spatially structured gold PSPP. Lower panel: The dynamics of the (LP,LP) diagonal and (LP,X)/(X,LP) cross peaks reveal pronounced Rabi oscillations with a period matching the peak splitting. Reproduced from [86]. CC BY 4.0.

Coherent oscillations are not limited to interactions between LP and UP. Timmer *et al* demonstrated that plasmonic electric fields can coherently drive population transfer between weakly and strongly coupled excitons located in spatially distinct regions of the sample (figure 4(c)) [86]. The investigated system consists of a gold nanoslit array coated with a thin film of squaraine-based J-aggregates. Using 2DES with varying angles of incident light, they explored polaritonic systems with different detuning conditions. Intriguingly, they found that while Rabi oscillations between LP and UP were evident at near-zero detuning, this behavior vanished in red-detuned systems. Instead, a new coherent oscillation emerged, with a frequency matching the energy difference between LP and a weakly coupled exciton state (X). The X excitons were situated in regions of the nanoslit array where the electric field was insufficiently strong to induce SC. Despite this, the experiments revealed that the strong local field enhancement in other regions of the nanoslit facilitated coherent energy transport to these X excitonic states, over mesoscopic distances. This plasmon-mediated coherence, observed even under ambient conditions, underscores its potential for practical room-temperature applications. Furthermore, these findings suggest that such coherent dynamics could significantly influence the optical and transport properties of polariton–exciton systems, anticipating the role of coherence in energy transport, which will be discussed in section 5.2.2.

5.1.1. The role of vibronic coupling

An emerging area of interest involves the interplay between polaritonic and vibronic coupling, giving rise to vibronic polariton states [48], as anticipated in section 2.4. In systems exhibiting strong vibronic coupling, electronic transitions interact with molecular vibrational modes, forming hybrid states with partially electronic character. In purely excitonic systems (without the cavity), vibronic coupling can lead to long-lived vibronic coherences [126, 127]. These coherences, which retain partial electronic character, have gained interest due to their potential role in influencing coherent dynamics and energy transfer mechanisms [128]. In analogy to what happens in purely excitonic systems, vibronic coupling plays a critical and multifaceted role in the polaritonic systems. This coupling is widely recognized for its capacity to reshape the polaritonic energy landscape strongly influencing both the coherent and the incoherent relaxation dynamics [48, 50, 51, 81, 129–139]. Traditionally, the coupling with vibrational modes has often been associated with decoherence, which leads to a reduction in coherence. This occurs because vibrational modes can disrupt the delicate

phase relationships necessary for maintaining coherent interactions between polaritons. In this context, when the Rabi splitting significantly exceeds the vibrational mode energy in regimes of strong light–matter coupling, polaron decoupling can mitigate these detrimental effects by isolating excitonic states from their vibrational environment (figure 1(f)) [49, 53, 55, 56]. This decoupling reduces the impact of molecular vibrations, thereby enhancing coherence within the polaritonic system. However, it must be underlined that the role of vibronic coupling is not limited to being a source of decoherence. Recent studies have shown that, under specific conditions, it can actively promote coherence by mediating the effective energy exchange and stabilizing coherence. For example, Nguyen *et al* have recently demonstrated that the coupling with low-frequency phonon modes can guide coherent intra-Rabi oscillations between bright and dark excitonic states in $CsPbBr_3$ halide perovskites [140]. Although not strictly polaritonic, this phenomenon emphasizes the non-trivial role of vibronic coupling in coherent dynamics and suggests analogies with polaritonic systems' behavior. Returning to vibronic polariton systems, Del Pino *et al*, using an approach where nuclear, electronic, and photonic processes are treated fully and on equal footing, theorized that vibronic coupling can mediate coherent population exchange between polaritonic states and DSs [131]. These dynamics are significantly influenced by multiphonon processes and non-Markovian effects. In addition, they revealed that these coherent vibration-driven oscillations are enhanced for Rabi frequencies in which vibronic and photonic couplings become comparable. This underscores the role of vibronic coupling in reshaping the dynamics and coherence of these hybrid light–matter states. This conclusion is further supported also by a recent research that explored the phonon-induced modifications in polaritonic Rabi oscillations under the influence of a dark excitonic condensate [133]. The authors propose a mechanism where phonons mediate bright–dark excitonic interconversion, significantly altering the standard polaritonic Rabi oscillations. Their findings emphasize that these interactions lead to unique polariton-like states involving photons, bright excitons, and phonons, collectively referred to as photon–exciton–phonon polaritons.

Taken together, these studies illustrate that the impact of vibronic coupling is highly context-dependent, shaped by many factors such as the strength of light–matter coupling, the vibrational modes' frequency, the strength of vibronic coupling, and the energy matching between all these states. While the field of research remains open, we believe that vibronic interactions can play a decisive role in shaping coherent dynamics, pointing to their potential as critical elements in the stabilization and control of polaritonic systems.

5.2. Macroscopic effects of coherent dynamics

The high dephasing rates in these systems often limit the direct observation of coherent phenomena. However, even when such dynamics are short-lived or challenging to detect, they can still significantly influence macroscopic properties such as ultra-long-range energy transfer, coherent polariton transport, or BEC, manifesting their effects without requiring direct observation of the underlying coherence.

5.2.1. Polariton assisted energy transfer

Energy transfer between a donor and an acceptor is a fundamental process in many natural and technological systems, playing a crucial role in fields such as photosynthesis, sensing, optoelectronics, and energy harvesting, just to cite a few. Traditionally, this transfer occurs through mechanisms such as FRET or Dexter energy transfer, which rely on dipole–dipole interactions or electron exchange, respectively. These classical mechanisms, however, are typically limited by the spatial separation between the donor and acceptor, with the efficiency decreasing significantly over longer distances. The advent of polaritonic systems offers an alternative and powerful approach to energy transfer [11]. A typical system consists of two exciton species (specifically, a donor and an acceptor), originating from different materials, and coupled to the same photonic cavity while being separated by a non-interacting spacer (figure 5(a)) [38]. As a result of SC, three distinct polaritonic states are formed: the UP, MP, and LPs (figure 5(c)). The UP primarily derives its excitonic contribution from the higher-energy exciton (the donor), whereas the LP is mainly influenced by the lower-energy exciton (the acceptor). In contrast, the MP exhibits a hybrid nature, incorporating contributions from both excitons [141, 142]. The highly delocalized nature of these polaritonic states across the entire cavity enables efficient energy flow between donor and acceptor species, facilitating energy transfer over mesoscopic distances and surpassing classical energy transfer processes, as demonstrated by numerous studies [11, 38, 143–146].

Initially, the role of quantum coherence in this mechanism was not explicitly mentioned but was often suggested indirectly through the concepts of delocalization and entanglement inherent in polaritonic states, which allow energy to be distributed more effectively across larger areas. Recently, Pajunpää *et al* performed a full quantum dynamics simulation to study polariton-assisted exciton population exchange dynamics [148]. In this work, the role of coherence in facilitating long-distance energy transfer was explicitly described. The simulation revealed how energy transfer was mediated through coherent oscillations of the donor and acceptor excitons' populations within the first 30 fs, mediated by cavity photons.

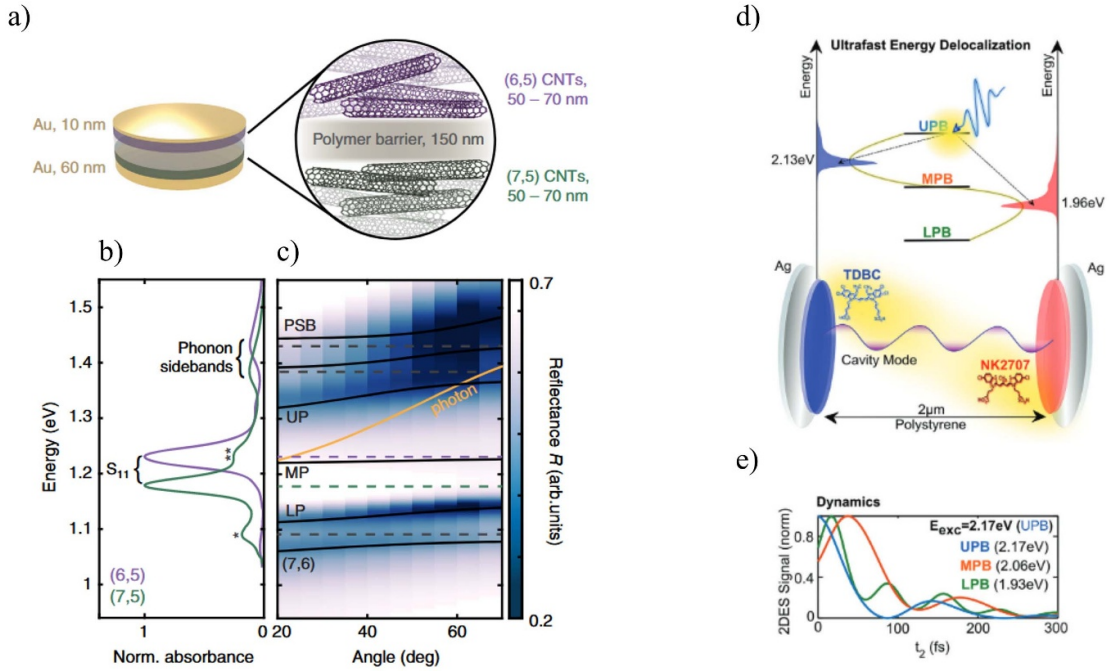

Figure 5. Polariton assisted energy transfer. (a) Schematic illustration of a mixed exciton–polariton system composed of carbon nanotubes embedded in a gold microcavity and separated through a 150 nm width polymer layer. (b) The absorption spectra of the two isolated excitonic systems and (c) the resulting anticrossing behavior where the LP, MP and UP states can be distinguished. (a)–(c) Reproduced from [38]. CC BY 4.0. (d) The hybrid polariton states can coherently connect different molecular species, even if separated by long distances. (e) Simulated population dynamics of the LP, MP and UP states after the excitation at the energy of UP. (d), (e) Reproduced from [147]. CC BY 4.0.

Key experimental evidence that explicitly highlights the role of coherence in polariton-assisted energy transfer was given by Russo *et al* [147]. In this work, 2DES was employed to demonstrate ultrafast energy delocalization between donor and acceptor molecules embedded in a strongly coupled microcavity. The experiment involved a 2-micron inert polystyrene spacer between layers of J-aggregate dyes, ensuring that the molecular excitons were spatially separated well beyond the Förster radius. This separation prevented energy transfer via conventional mechanisms like FRET, thereby emphasizing the necessity of polaritonic pathways for such long-distance energy transfer. The results revealed that polaritons facilitated ultrafast energy redistribution across the entire system, with energy moving coherently between spatially distant donor and acceptor states (figure 5(d)). This phenomenon was observed as an almost instantaneous energy transfer between polariton states, manifested by cross-peaks in the 2DES maps at extremely short timescales (∼20 fs). To gain further insight into this process, the authors simulated the 2DES signal using a fully coherent, broadband model for polaritons. The model predicted that, in the absence of dephasing processes, coherent oscillations between the different polariton modes dominated the population dynamics, akin to Rabi oscillations observed in strongly coupled systems (figure 5(e)). These oscillations were crucial in explaining how energy became delocalized over large distances upon excitation of a donor state, enabling efficient energy transfer not achievable by classical pathways.

In summary, these works demonstrate that polariton-assisted energy transfer opens new possibilities for controlling energy flow at the nanoscale, where the coherent properties of polaritons can be harnessed to design systems with enhanced energy transfer efficiency over extended distances. Such advances could have significant implications for the design of next-generation optoelectronic devices, artificial photosynthetic systems, and quantum technologies, where coherent energy dynamics play a pivotal role.

5.2.2. Coherent polariton transport

Excitonic transport is fundamental in numerous physical and technological applications, including photosynthesis, optoelectronics, and energy conversion. However, the inherently disordered nature of organic and semiconductor materials often limits excitonic transport to predominantly diffusive regimes. These regimes are characterized by random hopping mechanisms mediated by phonons or local Coulombic interactions, resulting in diffusion lengths of only a few nanometers. This poses significant challenges for applications requiring energy transfer over longer distances. By leveraging SC between excitons and confined photons, it is possible to bypass these limitations, combining the coherence and delocalization of photons

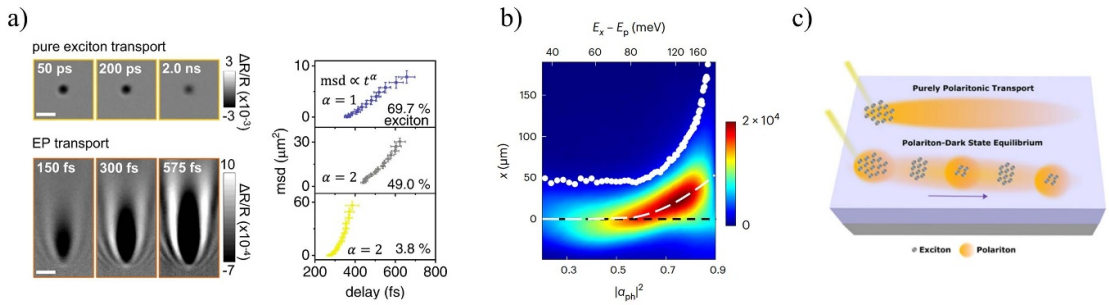

Figure 6. Coherent polariton transport. (a) Left panel: slow and diffusive propagation of a pure exciton compared with the coherent propagation of an exciton–polariton observed through a momentum-resolved real-time imaging microscopy. Right panel: transition from diffusive transport of polaritons with high excitonic character to ballistic transport of polaritons with excitonic character $\leqslant$ 49%. Reproduced from [151]. CC BY 4.0. (b) Steady-state spatial emission distribution of LP as a function of its photonic character reveals its strong influence on the polariton transport. By tuning the excitonic–photonic character, it is possible to reach coherent propagation covering distances up to 100 μm. Reproduced from [152], with permission from Springer Nature. (c) Schematic representation of purely polariton transport (top) and polariton transport mediated through the equilibrium with DSs (bottom). Reproduced from [5]. CC BY 4.0.

with the interactive features of excitons. This was demonstrated showing that polaritons can propagate ballistically (coherently) over hundreds of micrometers in high-quality Fabry–Pérot and microcavity systems, highlighting their potential to overcome diffusive transport limits [108, 149, 150]. Recent research has further expanded this understanding by identifying mechanisms for transitions between diffusive and ballistic regimes [151, 152], the critical role of DSs and energetic disorder in the mechanism [31, 33–37, 39, 153, 154], and the influence of cavity design and material properties in optimizing and tuning polariton transport [10, 39, 72, 149, 151, 153, 155–161]. These works highlight the versatility of polaritonic systems in achieving coherent transport at room temperature, even under highly disordered or challenging conditions.

In these studies, coherence emerges as the central property enabling such extended transport, emphasizing the importance of minimizing losses and balancing the photonic and excitonic contributions. In fact, the transition between diffusive and coherent transport regimes in polariton systems was demonstrated to be primarily governed by the excitonic–photonic composition of the polaritons [151, 152]. Xu *et al* used a momentum-resolved real-time imaging microscopy in high-quality inorganic microcavities to observe the propagation of polaritons (figure 6(a), left). A systematic study revealed that polaritons with high photonic fractions ($\geqslant$50%) exhibit ballistic transport, characterized by coherent propagation at speeds approaching the velocity of light [151]. In contrast, as the excitonic fraction increases, the incoherent scattering with phonons significantly reduces the coherence, driving the transition to diffusive transport (figure 6(a), right). Complementary, Balasubrahmaniyam *et al* (figure 6(b)) examined polaritonic transport in organic J-aggregates strongly coupled with BSWs, demonstrating an enhancement of excitonic diffusion by up to six orders of magnitude compared to bare excitons. Furthermore, they captured the transition to coherent propagation at high photonic fractions, characterized by speeds reaching two-thirds the speed of light and transport distances of up to 100 μm [152]. However, for polaritonic transport to be viable in functional devices, it is crucial that a significant fraction of the excitation is effectively transported, which presents a new challenge in maintaining ballistic transport while preserving a high excitonic character [155].

The strength of polariton transport emerges also in disorder materials, where the coherence induced by the photonic component mitigates the effects of molecular inhomogeneity, enabling energy transfer even in challenging environments, extending the transport length by several orders of magnitude compared to conventional excitonic diffusion [72]. In addition, recent insights into the nature of DSs in disordered systems highlight their significant contribution to polariton transport mechanisms. As discussed in section 2.3, Botzung *et al* theoretically demonstrated the semilocalized nature of DSs and their role in supporting coherent transport [31, 33]. Building on this, other theoretical studies have explored the interplay between DSs and energetic disorder, further emphasizing their critical role in facilitating long-range energy transport mechanisms [33–37]. Therefore, while polaritons can exhibit a range of transport behaviors, from enhanced diffusive to ballistic propagation, DSs display a diffusive, exciton-like transport, which can be influenced by their non-localized nature. In addition, the possibility of ultrafast energy exchange between polaritonic states and DSs creates a scenario where polariton transport remains ballistic (as long as it maintains a sufficient photonic character) but with a reduced velocity if compared to the predicted group velocity. In this context, DSs play a dual role: they act as a brake, reducing the transport velocity due to the fraction of time the population spends in the dark manifold, while simultaneously serving as a reservoir, enabling the regeneration of highly propagating polaritons. This was experimentally observed by Pandya *et al*

[39]. This work observed an increase in polariton transport velocity when using cavities with a higher *Q*-factor. This was attributed to an enhancement in the DSs' delocalization induced by the cavity, facilitating the fast (<100 fs) energy exchange between DSs and polaritonic states, ultimately leading to higher transport velocities. This hybrid mechanism of propagation was supported by the work of Jin *et al*, who emphasized the critical role of interactions between DSs and polaritons in mediating propagation in diffusive regimes [153]. In contrast, the work conducted by Xu *et al* shows ballistic polariton propagation with group velocities consistent with theory, which are only affected by phonon-scattering interactions, suggesting a purely polaritonic transport [151]. These contrasting results highlight the coexistence of two different transport regimes: the purely polaritonic transport (figure 6(c), top) and the DSs mediated transport (figure 6(c), bottom) [153]. Disentangling one mechanism from the other and determining the conditions under which each prevails remains an open challenge [5]. A possible approach to achieve that is to modulate the energy exchange between DSs and polaritonic states and analyze the resulting changes in transport properties [39]. Additionally, a coherent transport lifetime significantly longer than the expected polariton lifetime could indicate a contribution from long-lived DSs. On the other hand, a polariton propagation velocity matching the predicted group velocity would suggest purely polaritonic transport [151].

Finally, the properties of coherent polariton transport strongly depend on the type of cavity and material. BSWs and Fabry–Pérot cavities enable precise control over polariton dispersion while minimizing photonic losses (and therefore extending transport lengths) through high *Q*-factors and tunable resonance conditions [59, 72, 150, 152, 156, 161]. Metasurfaces of perovskites, as explored by Dang *et al* [155] provide coherent propagation of polaritons with excitonic fraction up to 80%. Using SLRs in plasmonic arrays offers a versatile and adaptable cavity system to enhance the exciton transport in the diffusive regime [153]. Hybrid plasmonic–photonic modes in periodic metallic structures can enable directional and ultralong (up to 600 μm) coherent energy transport [158, 159]. Bare organic semiconductors, without needing an external cavity, can host microcavity-like exciton–polaritons that dominate photoexcitation dynamics and enable efficient energy propagation [160].

5.2.3. Polariton condensation

Another striking manifestation of macroscopic coherence in hybrid exciton–polariton systems arises from the bosonic nature of photons and excitons, which are governed by Bose–Einstein statistics. Under specific conditions, bosonic particles can collectively occupy the system's lowest energy state (LP in polariton systems), forming what is known as a BEC [8]. This LP state occupation leads to the emergence of collective quantum states, where coherence spans both spatial and temporal domains, fundamentally altering the system's dynamics. While a detailed discussion of this phenomenon is beyond the scope of this review, interested readers are directed to other excellent, dedicated reviews [46, 64, 162].

It is worth emphasizing that, while BEC is traditionally described under thermodynamic equilibrium conditions [163], the short lifetime of exciton–polaritons, relative to their thermalization time, often leads to the formation of nonequilibrium condensation. In this condition, the exciton–polariton condensation is considered an out-of-equilibrium process maintained through a dynamic balance of pumping and dissipation. However, in some cases, exciton–polariton condensation can reach thermal equilibrium if the polariton lifetime is sufficiently long [164–166], opening up a new perspective on exciton–polariton condensation [167]. One of the key advantages of exciton–polariton condensation over conventional BEC lies in the critical temperature for condensation, which inversely depends on the effective mass of the bosons. In fact, due to their exceptionally low effective mass and bosonic nature, exciton–polaritons can condense at significantly higher temperatures [8, 46]. This advantage is further enhanced by the high binding energy of Frenkel excitons in organic exciton–polaritons [168–170], or the extended lifetimes of polaritons in inorganic systems [165, 171], allowing critical temperatures to reach even room temperature.

The formation of polariton condensation critically depends on the scattering processes from the ER into the LP state, as well as its lifetime (figure 7). As discussed in section 4, the primary mechanisms facilitating this transition are radiative pumping and VAS [1, 5, 93, 97–103]. Notably, the vibronic coupling (discussed in sections 2.4 and 5.1.1) has been shown to play a decisive role in driving the polarization condensation, highlighting how vibronic interactions could directly contribute to establishing macroscopic coherence [102]. Evidence of polariton condensates is provided by long-range spatial and temporal coherence, hallmark features of macroscopic quantum states that have been confirmed through interference experiments and time-resolved measurements [8, 172]. Another key manifestation of exciton–polariton condensation is the emergence of laser-like emission, which is associated with the radiative transition from the LP to the GS, namely, polariton lasing (figure 7) [63, 170, 171, 173]. Unlike conventional photon lasers, this emission does not rely on population inversion. Instead, polariton lasing is driven by stimulated scattering into the LP state, enabling much lower lasing thresholds. At the condensation threshold, the emission intensity experiences a sharp increase, accompanied by significant spectral narrowing, indicative of the onset of coherence. This

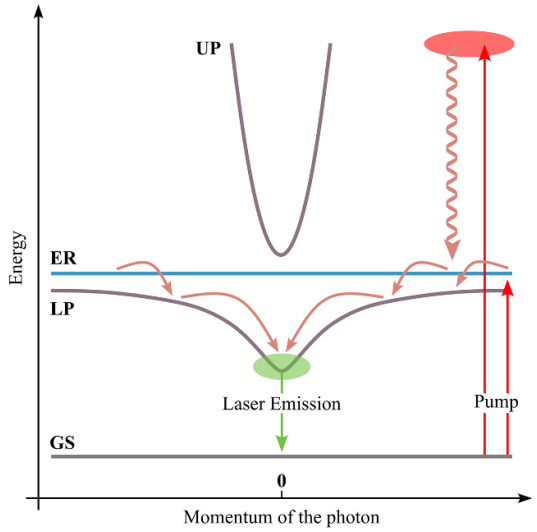

Figure 7. Polariton condensation. Mechanism of polariton condensation: the pump laser (red arrows) initially excites the exciton reservoir (non-resonantly or resonantly) which then scatters to the bottom of the LP through mechanisms such as radiative pumping and VAS. The accumulation of polaritons at zero momentum leads to stimulated emission, resulting in polariton lasing.

behavior is often accompanied by a power-dependent blue-shift, which is attributed to polariton–polariton interactions and changes in the ER, reflecting the nonlinear dynamics that are intrinsic to polariton condensates [174].

Beyond polariton lasing, polariton condensates offer transformative potential in photonic and quantum technologies, driven by their macroscopic coherence. This coherence enables quantum phenomena such as superfluidity, characterized by frictionless flow and minimal dissipation [9], and vorticity, [175] making them ideal for ultra-efficient photonic circuits and energy-saving communication systems [176]. The nonlinear optical response of polaritons supports ultrafast all-optical switches and logic gates, essential for next-generation photonic processors [58, 177]. These systems achieve unparalleled speed and energy efficiency by leveraging strong polariton interactions, eliminating the need for electronic intermediaries. Additionally, their coherence facilitates applications in quantum technologies, such as the generation of entangled photons and quantum memories, enabling robust quantum communication networks and scalable quantum information storage [178, 179].

6. Conclusions and perspectives

Exciton–polariton systems have emerged as a versatile platform at the crossroads of fundamental quantum science and practical applications. Among other valuable properties, their unique ability to sustain quantum coherence on macroscopic scales, combined with the interplay between light and matter properties, makes them invaluable for exploring coherent phenomena. These hybrid quasiparticles offer both a deeper understanding of quantum phenomena and a foundation for transformative technologies in quantum computing, photonics, and energy harvesting. This review highlighted the great scientific interest and advancements in the observation and utilization of coherent phenomena, including Rabi oscillations, long-distance coherent energy transfer, ballistic energy transport in surface materials, and BEC.

Despite significant progress, challenges remain in fully harnessing the potential of exciton–polariton systems. A key difficulty lies in enhancing and maintaining the delicate coherence that defines their unique properties. Energetic disorder, vibrational coupling, and dissipation can disrupt coherence, alter energy transfer pathways, and introduce complex relaxation mechanisms. Addressing these challenges demands ongoing improvements in experimental techniques and theoretical models capable of capturing the intricate interplay between coherence and dissipation. On the one hand, recent advancements in ultrafast spectroscopy and spatially resolved imaging have been pivotal in uncovering polaritonic coherent behavior. On the other hand, advances in QEDs models have greatly improved the simulation of polaritonic systems, incorporating phenomena such as disorder, vibronic coupling, and non-Markovian dynamics. These models not only deepen our understanding but also aid in designing polariton-based devices with optimized performance.

In conclusion, exciton–polariton systems represent a dynamic and rapidly evolving field at the intersection of fundamental physics and applied science. By addressing current challenges and leveraging new experimental and theoretical tools, the scientific community is poised to unlock the full potential of

these hybrid quasiparticles, paving the way for groundbreaking advances in quantum science and transformative technologies.

Data availability statement

No new data were created or analysed in this study.

Acknowledgment

This research was funded by the European Union—Next Generation EU, Mission 4 Component 1 CUP C53D23003810006 (PRIN project 'CHI-EP') and supported by the P-DiSC#04BIRD2022-UNIPD Grant.

ORCID iDs

Federico Toffoletti https://orcid.org/0009-0007-7733-4593
Elisabetta Collini https://orcid.org/0000-0002-1019-9100

References

[1] Bhuyan R, Mony J, Kotov O, Castellanos G W, Gómez Rivas J, Shegai T O and Börjesson K 2023 The rise and current status of polaritonic photochemistry and photophysics *Chem. Rev.* **123** 10877–919
[2] Törmä P and Barnes W L 2015 Strong coupling between surface plasmon polaritons and emitters: a review *Rep. Prog. Phys.* **78** 013901
[3] Ebbesen T W 2016 Hybrid light–matter states in a molecular and material science perspective *Acc. Chem. Res.* **49** 2403–12
[4] Low T, Chaves A, Caldwell J D, Kumar A, Fang N X, Avouris P, Heinz T F, Guinea F, Martin-Moreno L and Koppens F 2017 Polaritons in layered two-dimensional materials *Nat. Mater.* **16** 182–94
[5] Khazanov T, Gunasekaran S, George A, Lomlu R, Mukherjee S and Musser A J 2023 Embrace the darkness: an experimental perspective on organic exciton–polaritons *Chem. Phys. Rev.* **4** 041305
[6] Hirai K, Hutchison J A and Uji-i H 2023 Molecular chemistry in cavity strong coupling *Chem. Rev.* **123** 8099–126
[7] Baranov D G, Wersäll M, Cuadra J, Antosiewicz T J and Shegai T 2018 Novel nanostructures and materials for strong light–matter interactions *ACS Photonics* **5** 24–42
[8] Kasprzak J *et al* 2006 Bose–Einstein condensation of exciton polaritons *Nature* **443** 409–14
[9] Amo A, Lefrère J, Pigeon S, Adrados C, Ciuti C, Carusotto I, Houdré R, Giacobino E and Bramati A 2009 Superfluidity of polaritons in semiconductor microcavities *Nat. Phys.* **5** 805–10
[10] Sandik G, Feist J, García-Vidal F J and Schwartz T 2024 Cavity-enhanced energy transport in molecular systems *Nat. Mater.* **24** 344–55
[11] Coles D M, Somaschi N, Michetti P, Clark C, Lagoudakis P G, Savvidis P G and Lidzey D G 2014 Polariton-mediated energy transfer between organic dyes in a strongly coupled optical microcavity *Nat. Mater.* **13** 712–9
[12] Dovzhenko D S, Ryabchuk S V, Rakovich P and Nabiev R I 2018 Light–matter interaction in the strong coupling regime: configurations, conditions, and applications *Nanoscale* **10** 3589–605
[13] Ribeiro R F, Martínez-Martínez L A, Du M, Campos-Gonzalez-Angulo J and Yuen-Zhou J 2018 Polariton chemistry: controlling molecular dynamics with optical cavities *Chem. Sci.* **9** 6325–39
[14] Pelton M, Storm S D and Leng H 2019 Strong coupling of emitters to single plasmonic nanoparticles: exciton-induced transparency and Rabi splitting *Nanoscale* **11** 14540–52
[15] Hertzog M, Wang M, Mony J and Börjesson K 2019 Strong light–matter interactions: a new direction within chemistry *Chem. Soc. Rev.* **48** 937–61
[16] Purcell E M 1995 Spontaneous emission probabilities at radio frequencies *Confined Electrons and Photons: New Physics and Applications* ed E Burstein and C Weisbuch (Springer US) pp 839
[17] Marquier F, Sauvan C and Greffet J-J 2017 Revisiting quantum optics with surface plasmons and plasmonic resonators *ACS Photonics* **4** 2091–101
[18] Hümmer T, García-Vidal F J, Martín-Moreno L and Zueco D 2013 Weak and strong coupling regimes in plasmonic QED *Phys. Rev.* B **87** 115419
[19] Krasnok A E, Slobozhanyuk A P, Simovski C R, Tretyakov S A, Poddubny A N, Miroshnichenko A E, Kivshar Y S and Belov P A 2015 An antenna model for the Purcell effect *Sci. Rep.* **5** 12956
[20] Jaynes E T and Cummings F W 1963 Comparison of quantum and semiclassical radiation theories with application to the beam maser *Proc. IEEE* **51** 89–109
[21] Takahashi S, Watanabe K and Matsumoto Y 2019 Singlet fission of amorphous rubrene modulated by polariton formation *J. Chem. Phys.* **151** 074703
[22] Scully M O and Zubairy M S 1997 *Quantum Optics* (Cambridge University Press) (https://doi.org/10.1017/CBO9780511813993)
[23] Tavis M and Cummings F W 1968 Exact solution for an N-Molecule—radiation-field Hamiltonian *Phys. Rev.* **170** 379–84
[24] Garraway B M 2011 The Dicke model in quantum optics: Dicke model revisited *Phil. Trans. R. Soc.* A **369** 1137–55
[25] Houdré R, Stanley R P and Ilegems M 1996 Vacuum-field Rabi splitting in the presence of inhomogeneous broadening: resolution of a homogeneous linewidth in an inhomogeneously broadened system *Phys. Rev.* A **53** 2711–5
[26] Ying W, Mondal M E and Huo P 2024 Theory and quantum dynamics simulations of exciton-polariton motional narrowing *J. Chem. Phys.* **161** 064105
[27] Climent C, Subotnik J E and Nitzan A 2024 Kubo-Anderson theory of polariton line shape *Phys. Rev.* A **109** 052809
[28] Sun K, Dou C, Gelin M F and Zhao Y 2022 Dynamics of disordered Tavis–Cummings and Holstein–Tavis–Cummings models *J. Chem. Phys.* **156** 024102
[29] Gera T and Sebastian K L 2022 Exact results for the Tavis–Cummings and Hückel Hamiltonians with diagonal disorder *J. Phys. Chem.* A **126** 5449–57

[30] Gera T and Sebastian K L 2022 Effects of disorder on polaritonic and dark states in a cavity using the disordered Tavis–Cummings model *J. Chem. Phys.* **156** 194304
[31] Botzung T, Hagenmüller D, Schütz S, Dubail J, Pupillo G and Schachenmayer J 2020 Dark state semilocalization of quantum emitters in a cavity *Phys. Rev.* B **102** 144202
[32] Evers F and Mirlin A D 2008 Anderson Transitions *Rev. Mod. Phys.* **80** 1355–417
[33] Dubail J, Botzung T, Schachenmayer J, Pupillo G and Hagenmüller D 2022 Large random arrowhead matrices: multifractality, semilocalization, and protected transport in disordered quantum spins coupled to a cavity *Phys. Rev.* A **105** 023714
[34] Allard T F and Weick G 2022 Disorder-enhanced transport in a chain of lossy dipoles strongly coupled to cavity photons *Phys. Rev.* B **106** 245424
[35] Chávez N C, Mattiotti F, Méndez-Bermúdez J A, Borgonovi F and Celardo G L 2021 Disorder-enhanced and disorder-independent transport with long-range hopping: application to molecular chains in optical cavities *Phys. Rev. Lett.* **126** 153201
[36] Engelhardt G and Cao J 2022 Unusual dynamical properties of disordered polaritons in microcavities *Phys. Rev.* B **105** 064205
[37] Engelhardt G and Cao J 2023 Polariton localization and dispersion properties of disordered quantum emitters in multimode microcavities *Phys. Rev. Lett.* **130** 213602
[38] Son M, Armstrong Z T, Allen R T, Dhavamani A, Arnold M S and Zanni M T 2022 Energy cascades in donor-acceptor exciton-polaritons observed by ultrafast two-dimensional white-light spectroscopy *Nat. Commun.* **13** 7305
[39] Pandya R, Ashoka A, Georgiou K, Sung J, Jayaprakash R, Renken S, Gai L, Shen Z, Rao A and Musser A J 2022 Tuning the coherent propagation of organic exciton-polaritons through dark state delocalization *Adv. Sci.* **9** 2105569
[40] George A, Geraghty T, Kelsey Z, Mukherjee S, Davidova G, Kim W and Musser A J 2024 Controlling the manifold of polariton states through molecular disorder *Adv. Opt. Mater.* **12** 2302387
[41] Fassioli F, Park K H, Bard S E and Scholes G D 2021 Femtosecond photophysics of molecular polaritons *J. Phys. Chem. Lett.* **12** 11444–59
[42] Gunasekaran S, Pinard R F and Musser A J 2024 Continuum model of strong light-matter coupling for molecular polaritons (arXiv:2308.08744)
[43] Wellnitz D, Pupillo G and Schachenmayer J 2022 Disorder enhanced vibrational entanglement and dynamics in polaritonic chemistry *Commun. Phys.* **5** 120
[44] Warnes J H, de Paula F M, Costa N C and de Sá Neto O P 2023 Dynamics of quantum coherence in the Jaynes–Cummings model with quenched disorder *Phys. Open* **15** 100146
[45] Scholes G D 2020 Polaritons and excitons: Hamiltonian design for enhanced coherence *Proc. R. Soc.* A **476** 20200278
[46] Deng H, Haug H and Yamamoto Y 2010 Exciton-polariton Bose-Einstein condensation *Rev. Mod. Phys.* **82** 1489–537
[47] Holmes R J and Forrest S R 2004 Strong exciton-photon coupling and exciton hybridization in a thermally evaporated polycrystalline film of an organic small molecule *Phys. Rev. Lett.* **93** 186404
[48] Herrera F and Spano F C 2018 Theory of nanoscale organic cavities: the essential role of vibration-photon dressed states *ACS Photonics* **5** 65–79
[49] Herrera F and Spano F C 2017 Absorption and photoluminescence in organic cavity QED *Phys. Rev.* A **95** 053867
[50] Deshmukh R, Marques P, Panda A, Sfeir M Y, Forrest S R and Menon V M 2020 Modifying the spectral weights of vibronic transitions via strong coupling to surface plasmons *ACS Photonics* **7** 43–48
[51] Avramenko A G and Rury A S 2022 Light emission from vibronic polaritons in coupled metalloporphyrin-multimode cavity systems *J. Phys. Chem. Lett.* **13** 4036–45
[52] Ćwik J A, Reja S, Littlewood P B and Keeling J 2014 Polariton condensation with saturable molecules dressed by vibrational modes *EPL* **105** 47009
[53] Herrera F and Spano F C 2016 Cavity-controlled chemistry in molecular ensembles *Phys. Rev. Lett.* **116** 238301
[54] Herrera F and Spano F C 2017 Dark vibronic polaritons and the spectroscopy of organic microcavities *Phys. Rev. Lett.* **118** 223601
[55] Takahashi S and Watanabe K 2020 Decoupling from a thermal bath via molecular polariton formation *J. Phys. Chem. Lett.* **11** 1349–56
[56] Spano F C 2015 Optical microcavities enhance the exciton coherence length and eliminate vibronic coupling in J-aggregates *J. Chem. Phys.* **142** 184707
[57] Bellessa J, Bloch J, Deleporte E, Menon V M, Nguyen H S, Ohadi H, Ravets S and Boulier T 2024 Materials for excitons–polaritons: exploiting the diversity of semiconductors *MRS Bull.* **49** 932–47
[58] Sanvitto D and Kéna-Cohen S 2016 The road towards polaritonic devices *Nat. Mater.* **15** 1061–73
[59] Zhou Z, Chen H-T, Sukharev M, Subotnik J E and Nitzan A 2024 Nature of polariton transport in a Fabry-Perot cavity *Phys. Rev.* A **109** 033717
[60] Fraser M D 2017 Coherent exciton-polariton devices *Semicond. Sci. Technol.* **32** 093003
[61] Greene R L, Bajaj K K and Phelps D E 1984 Energy levels of Wannier excitons in GaAs–$Ga_{1-x}Al_xAs$ quantum-well structures *Phys. Rev.* B **29** 1807–12
[62] Ardizzone V, Marco L D, Giorgi M D, Dominici L, Ballarini D and Sanvitto D 2019 Emerging 2D materials for room-temperature polaritonics *Nanophotonics* **8** 1547–58
[63] Schneider C *et al* 2013 An electrically pumped polariton laser *Nature* **497** 348–52
[64] Byrnes T, Kim N Y and Yamamoto Y 2014 Exciton–polariton condensates *Nat. Phys.* **10** 803–13
[65] Sun Z *et al* 2017 Optical control of room-temperature valley polaritons *Nat. Photon.* **11** 491–6
[66] Zhao J, Fieramosca A, Bao R, Dini K, Su R, Sanvitto D, Xiong Q and Liew T C H 2024 Room temperature polariton spin switches based on Van Der Waals superlattices *Nat. Commun.* **15** 7601
[67] Rahimi-Iman A 2020 Optical microcavities for polariton studies *Polariton Physics: From Dynamic Bose–Einstein Condensates in Strongly-Coupled Light–Matter Systems to Polariton Lasers* ed A Rahimi-Iman (Springer) pp 119–37
[68] Vasa P, Wang W, Pomraenke R, Lammers M, Maiuri M, Manzoni C, Cerullo G and Lienau C 2013 Real-time observation of ultrafast Rabi oscillations between excitons and plasmons in metal nanostructures with J-aggregates *Nat. Photon.* **7** 128–32
[69] Peruffo N, Gil G, Corni S, Mancin F and Collini E 2021 Selective switching of multiple plexcitons in colloidal materials: directing the energy flow at the nanoscale *Nanoscale* **13** 6005–15
[70] Zhang L, Gogna R, Burg W, Tutuc E and Deng H 2018 Photonic-crystal exciton-polaritons in monolayer semiconductors *Nat. Commun.* **9** 713
[71] Anantharaman S B *et al* 2025 Ultrastrong light–matter coupling in two-dimensional metal–organic chalcogenolates *Nat. Photon.* **19** 1–7

[72] Hou S, Khatoniar M, Ding K, Qu Y, Napolov A, Menon V M and Forrest S R 2020 Ultralong-range energy transport in a disordered organic semiconductor at room temperature via coherent exciton-polariton propagation *Adv. Mater.* **32** 2002127
[73] Lee Y-C, Ho Y-L, Lin B-W, Chen M-H, Xing D, Daiguji H and Delaunay J-J 2023 High-Q lasing via all-dielectric Bloch-surface-wave platform *Nat. Commun.* **14** 6458
[74] Barachati F, Fieramosca A, Hafezian S, Gu J, Chakraborty B, Ballarini D, Martinu L, Menon V, Sanvitto D and Kéna-Cohen S 2018 Interacting polariton fluids in a monolayer of tungsten disulfide *Nat. Nanotechnol.* **13** 906–9
[75] Bajoni D, Gerace D, Galli M, Bloch J, Braive R, Sagnes I, Miard A, Lemaître A, Patrini M and Andreani L C 2009 Exciton polaritons in two-dimensional photonic crystals *Phys. Rev.* B **80** 201308
[76] Su R, Fieramosca A, Zhang Q, Nguyen H S, Deleporte E, Chen Z, Sanvitto D, Liew T C H and Xiong Q 2021 Perovskite semiconductors for room-temperature exciton-polaritonics *Nat. Mater.* **20** 1315–24
[77] Canales A, Baranov D G, Antosiewicz T J and Shegai T 2021 Abundance of cavity-free polaritonic states in resonant materials and nanostructures *J. Chem. Phys.* **154** 024701
[78] Anantharaman S B, Jo K and Jariwala D 2021 Exciton–photonics: from fundamental science to applications *ACS Nano* **15** 12628–54
[79] Streltsov A, Adesso G and Plenio M B 2017 Colloquium: quantum coherence as a resource *Rev. Mod. Phys.* **89** 041003
[80] Heinrich A J, Oliver W D, Vandersypen L M K, Ardavan A, Sessoli R, Loss D, Jayich A B, Fernandez-Rossier J, Laucht A and Morello A 2021 Quantum-Coherent nanoscience *Nat. Nanotechnol.* **16** 1318–29
[81] Rouse D M, Gauger E M and Lovett B W 2024 Influence of strong molecular vibrations on decoherence of molecular polaritons *ACS Photonics* **11** 5215–28
[82] Chng B X K, Ying W, Lai Y, Vamivakas A N, Cundiff S T, Krauss T D and Huo P 2024 Mechanism of molecular polariton decoherence in the collective light–matter couplings regime *J. Phys. Chem. Lett.* **15** 11773–83
[83] Dhamija S and Son M 2024 Mapping the dynamics of energy relaxation in exciton–polaritons using ultrafast two-dimensional electronic spectroscopy *Chem. Phys. Rev.* **5** 041309
[84] Peruffo N, Mancin F and Collini E 2023 Coherent dynamics in solutions of colloidal plexcitonic nanohybrids at room temperature *Adv. Opt. Mater.* **11** 2203010
[85] Finkelstein-Shapiro D, Mante P-A, Sarisozen S, Wittenbecher L, Minda I, Balci S, Pullerits T and Zigmantas D 2021 Understanding radiative transitions and relaxation pathways in plexcitons *Chem* **7** 1092–107
[86] Timmer D *et al* 2023 Plasmon mediated coherent population oscillations in molecular aggregates *Nat. Commun.* **14** 8035
[87] Mewes L, Wang M, Ingle R A, Börjesson K and Chergui M 2020 Energy relaxation pathways between light-matter states revealed by coherent two-dimensional spectroscopy *Commun. Phys.* **3** 157
[88] Paul J, Rose H, Swagel E, Meier T, Wahlstrand J K and Bristow A D 2022 Coherent contributions to population dynamics in a semiconductor microcavity *Phys. Rev.* B **105** 115307
[89] Tang Y, Zhang Y, Liu Q, Wei K, Cheng X, Shi L and Jiang T 2022 Interacting plexcitons for designed ultrafast optical nonlinearity in a monolayer semiconductor *Light Sci. Appl.* **11** 94
[90] Agranovich V M, Litinskaia M and Lidzey D G 2003 Cavity polaritons in microcavities containing disordered organic semiconductors *Phys. Rev.* B **67** 085311
[91] Virgili T, Coles D, Adawi A M, Clark C, Michetti P, Rajendran S K, Brida D, Polli D, Cerullo G and Lidzey D G 2011 Ultrafast polariton relaxation dynamics in an organic semiconductor microcavity *Phys. Rev.* B **83** 245309
[92] Kuttruff J *et al* 2023 Sub-picosecond collapse of molecular polaritons to pure molecular transition in plasmonic photoswitch-nanoantennas *Nat. Commun.* **14** 3875
[93] Groenhof G, Climent C, Feist J, Morozov D and Toppari J J 2019 Tracking polariton relaxation with multiscale molecular dynamics simulations *J. Phys. Chem. Lett.* **10** 5476–83
[94] Melnikau D, Esteban R, Savateeva D, Sánchez-Iglesias A, Grzelczak M, Schmidt M K, Liz-Marzán L M, Aizpurua J and Rakovich Y P 2016 Rabi splitting in photoluminescence spectra of hybrid systems of gold nanorods and J-aggregates *J. Phys. Chem. Lett.* **7** 354–62
[95] Ceccarelli S, Wenus J, Skolnick M S and Lidzey D G 2007 Temperature dependent polariton emission from strongly coupled organic semiconductor microcavities *Superlattices Microstruct.* **41** 289–92
[96] Coles D M, Michetti P, Clark C, Adawi A M and Lidzey D G 2011 Temperature dependence of the upper-branch polariton population in an organic semiconductor microcavity *Phys. Rev.* B **84** 205214
[97] Hulkko E, Pikker S, Tiainen V, Tichauer R H, Groenhof G and Toppari J J 2021 Effect of molecular stokes shift on polariton dynamics *J. Chem. Phys.* **154** 154303
[98] Coles D M, Michetti P, Clark C, Tsoi W C, Adawi A M, Kim J and Lidzey D G 2011 Vibrationally assisted polariton-relaxation processes in strongly coupled organic-semiconductor microcavities *Adv. Funct. Mater.* **21** 3691–6
[99] Lodden G H and Holmes R J 2010 Electrical excitation of microcavity polaritons by radiative pumping from a weakly coupled organic semiconductor *Phys. Rev.* B **82** 125317
[100] Sasaki Y, Georgiou K, Wang S, Bossanyi D, Jayaprakash R, Yanai N, Kimizuka N, Lidzey D, Musser A and Clark J 2024 Radiative pumping in a strongly coupled microcavity filled with a neat molecular film showing excimer emission *Phys. Chem. Chem. Phys.* **26** 14745–53
[101] Grant R T *et al* 2016 Efficient radiative pumping of polaritons in a strongly coupled microcavity by a fluorescent molecular dye *Adv. Opt. Mater.* **4** 1615–23
[102] Ramezani M, Halpin A, Wang S, Berghuis M and Rivas J G 2019 Ultrafast dynamics of nonequilibrium organic exciton–polariton condensates *Nano Lett.* **19** 8590–6
[103] Tichauer R H, Morozov D, Sokolovskii I, Toppari J J and Groenhof G 2022 Identifying vibrations that control non-adiabatic relaxation of polaritons in strongly coupled molecule–cavity systems *J. Phys. Chem. Lett.* **13** 6259–67
[104] Zasedatelev A V, Baranikov A V, Urbonas D, Scafirimuto F, Scherf U, Stöferle T, Mahrt R F and Lagoudakis P G 2019 A room-temperature organic polariton transistor *Nat. Photon.* **13** 378–83
[105] Wei H, Yan X, Niu Y, Li Q, Jia Z and Xu H 2021 Plasmon–exciton interactions: spontaneous emission and strong coupling *Adv. Funct. Mater.* **31** 2100889
[106] Wersäll M, Munkhbat B, Baranov D G, Herrera F, Cao J, Antosiewicz T J and Shegai T 2019 Correlative dark-field and photoluminescence spectroscopy of individual plasmon–molecule hybrid nanostructures in a strong coupling regime *ACS Photonics* **6** 2570–6
[107] Lidzey D G, Bradley D D C, Virgili T, Armitage A, Skolnick M S and Walker S 1999 Room temperature polariton emission from strongly coupled organic semiconductor microcavities *Phys. Rev. Lett.* **82** 3316–9

[108] Rozenman G G, Akulov K, Golombek A and Schwartz T 2018 Long-range transport of organic exciton-polaritons revealed by ultrafast microscopy *ACS Photonics* **5** 105–10
[109] Schwartz T, Hutchison J A, Léonard J, Genet C, Haacke S and Ebbesen T W 2013 Polariton dynamics under strong light–molecule coupling *ChemPhysChem* **14** 125–31
[110] Scholes G D, DelPo C A and Kudisch B 2020 Entropy reorders polariton states *J. Phys. Chem. Lett.* **11** 6389–95
[111] Michail E, Rashidi K, Liu B, He G, Menon V M and Sfeir M Y 2024 Addressing the dark state problem in strongly coupled organic exciton-polariton systems *Nano Lett.* **24** 557–65
[112] Lee I, Melton S R, Xu D and Delor M 2024 Controlling molecular photoisomerization in photonic cavities through polariton funneling *J. Am. Chem. Soc.* **146** 9544–53
[113] Climent C, Casanova D, Feist J and Garcia-Vidal F J 2022 Not dark yet for strong light-matter coupling to accelerate singlet fission dynamics *Cr-phys-sc* **3** 4
[114] Mandal A, Taylor M A D, Weight B M, Koessler E R, Li X and Huo P 2023 Theoretical advances in polariton chemistry and molecular cavity quantum electrodynamics *Chem. Rev.* **123** 9786–879
[115] Tserkezis C, Fernández-Domínguez A I, Gonçalves P A D, Todisco F, Cox J D, Busch K, Stenger N, Bozhevolnyi S I, Mortensen N A and Wolff C 2020 On the applicability of quantum-optical concepts in strong-coupling nanophotonics *Rep. Prog. Phys.* **83** 082401
[116] Stete F, Bargheer M and Koopman W 2023 Ultrafast dynamics in plasmon–exciton core–shell systems: the role of heat *Nanoscale* **15** 16307–13
[117] Dominici L *et al* 2014 Ultrafast control and Rabi oscillations of polaritons *Phys. Rev. Lett.* **113** 226401
[118] Norris T B, Rhee J-K, Sung C-Y, Arakawa Y, Nishioka M and Weisbuch C 1994 Time-resolved vacuum Rabi oscillations in a semiconductor quantum microcavity *Phys. Rev.* B **50** 14663–6
[119] Wang Z, Gogna R and Deng H 2017 What is the best planar cavity for maximizing coherent exciton-photon coupling *Appl. Phys. Lett.* **111** 061102
[120] Hu W, Gustin I, Krauss T D and Franco I 2022 Tuning and enhancing quantum coherence time scales in molecules via light-matter hybridization *J. Phys. Chem. Lett.* **13** 11503–11
[121] Orfanakis K, Tzortzakakis A F, Petrosyan D, Savvidis P G and Ohadi H 2021 Ultralong temporal coherence in optically trapped exciton-polariton condensates *Phys. Rev.* B **103** 235313
[122] Brune Y, Rozas E, West K, Baldwin K, Pfeiffer L N, Beaumariage J, Alnatah H, Snoke D W and Aßmann M 2024 Quantum coherence of a long-lifetime exciton-polariton condensate (arXiv:2407.00844)
[123] Chong Y D, Ge L, Cao H and Stone A D 2010 Coherent perfect absorbers: time-reversed lasers *Phys. Rev. Lett.* **105** 053901
[124] Zanotto S, Mezzapesa F P, Bianco F, Biasiol G, Baldacci L, Vitiello M S, Sorba L, Colombelli R and Tredicucci A 2014 Perfect energy-feeding into strongly coupled systems and interferometric control of polariton absorption *Nat. Phys.* **10** 830–4
[125] Lai Y *et al* 2024 Room-temperature quantum nanoplasmonic coherent perfect absorption *Nat. Commun.* **15** 6324
[126] Sayers C J *et al* 2023 Strong coupling of coherent phonons to excitons in semiconducting monolayer $MoTe_2$ *Nano Lett.* **23** 9235–42
[127] Hüter O, Sala M, Neumann H, Zhang S, Studzinski H, Egorova D and Temps F 2016 Long-lived coherence in pentafluorobenzene as a probe of $\Pi\pi^*$—$\Pi\sigma^*$ vibronic coupling *J. Chem. Phys.* **145** 014302
[128] Sio A D, Nguyen X T and Lienau C 2019 Signatures of strong vibronic coupling mediating coherent charge transfer in two-dimensional electronic spectroscopy *Z. Naturforsch.* A **74** 721–37
[129] Galego J, Garcia-Vidal F J and Feist J 2015 Cavity-induced modifications of molecular structure in the strong-coupling regime *Phys. Rev.* X **5** 041022
[130] Ćwik J A, Kirton P, De Liberato S and Keeling J 2016 Excitonic spectral features in strongly coupled organic polaritons *Phys. Rev.* A **93** 033840
[131] Del Pino J, Schröder F A Y N, Chin A W, Feist J and Garcia-Vidal F J 2018 Tensor network simulation of non-Markovian dynamics in organic polaritons *Phys. Rev. Lett.* **121** 227401
[132] Kansanen K S U, Asikainen A, Toppari J J, Groenhof G and Heikkilä T T 2019 Theory for the stationary polariton response in the presence of vibrations *Phys. Rev.* B **100** 245426
[133] Alkady A, Fleurov V and Kuklov A 2025 Phonon-Induced modification of polaritonic Rabi oscillations in the presence of dark excitonic condensate *Phys. Rev.* B **111** 035201
[134] Hou E, Sun K, Gelin M F and Zhao Y 2024 Finite temperature dynamics of the Holstein–Tavis–Cummings model *J. Chem. Phys.* **160** 084116
[135] Liu J, Zhao Q and Wu N 2019 Vibration-assisted exciton transfer in molecular aggregates strongly coupled to confined light fields *J. Chem. Phys.* **150** 105102
[136] Zhang B and Liang W 2020 The vibronic absorption spectra and exciton dynamics of plasmon-exciton hybrid systems in the regimes ranged from fano antiresonance to Rabi-like splitting *J. Chem. Phys.* **152** 014102
[137] Latini S, De Giovannini U, Sie E J, Gedik N, Hübener H and Rubio A 2021 Phonoritons as hybridized exciton-photon-phonon excitations in a monolayer h -BN optical cavity *Phys. Rev. Lett.* **126** 227401
[138] Osipov V A and Fainberg B 2023 Hartree method for molecular polaritons *Phys. Rev.* B **107** 075404
[139] Zhang Z, Nie X, Lei D and Mukamel S 2023 Multidimensional coherent spectroscopy of molecular polaritons: Langevin approach *Phys. Rev. Lett.* **130** 103001
[140] Nguyen X T *et al* 2023 Phonon-driven intra-exciton Rabi oscillations in $CsPbBr_3$ halide perovskites *Nat. Commun.* **14** 1047
[141] Lidzey D G, Bradley D D C, Armitage A, Walker S and Skolnick M S 2000 Photon-mediated hybridization of Frenkel excitons in organic semiconductor microcavities *Science* **288** 1620–3
[142] Lidzey D G, Bradley D D C, Skolnick M S and Walker S 2001 Optical coupling of Frenkel excitons in organic semiconductor microcavities *Synth. Met.* **124** 37–40
[143] Garcia-Vidal F J and Feist J 2017 Long-distance operator for energy transfer *Science* **357** 1357–8
[144] Zhong X, Chervy T, Zhang L, Thomas A, George J, Genet C, Hutchison J A and Ebbesen T W 2017 Energy transfer between spatially separated entangled molecules *Angew. Chem., Int. Ed.* **56** 9034–8
[145] Du M, Martínez-Martínez L A, Ribeiro R F, Hu Z, Menon V M and Yuen-Zhou J 2018 Theory for polariton-assisted remote energy transfer *Chem. Sci.* **9** 6659–69
[146] Georgiou K, Jayaprakash R, Othonos A and Lidzey D G 2021 Ultralong-range polariton-assisted energy transfer in organic microcavities *Angew. Chem.* **133** 16797–803
[147] Russo M, Georgiou K, Genco A, De Liberato S, Cerullo G, Lidzey D G, Othonos A, Maiuri M and Virgili T 2024 Direct evidence of ultrafast energy delocalization between optically hybridized j-aggregates in a strongly coupled microcavity *Adv. Opt. Mater.* **12** 2400821

[148] Pajunpää T, Nigmatulin F, Akkanen S-T, Fernandez H, Groenhof G and Sun Z 2024 Polariton-assisted long-distance energy transfer between excitons in two-dimensional semiconductors *Phys. Rev.* B **109** 195409
[149] Steger M, Liu G, Nelsen B, Gautham C, Snoke D W, Balili R, Pfeiffer L and West K 2013 Long-range ballistic motion and coherent flow of long-lifetime polaritons *Phys. Rev.* B **88** 235314
[150] Lerario G *et al* 2016 High-speed flow of interacting organic polaritons *Light Sci. Appl.* **6** e16212
[151] Xu D, Mandal A, Baxter J M, Cheng S-W, Lee I, Su H, Liu S, Reichman D R and Delor M 2023 Ultrafast imaging of polariton propagation and interactions *Nat. Commun.* **14** 3881
[152] Balasubrahmaniyam M, Simkhovich A, Golombek A, Sandik G, Ankonina G and Schwartz T 2023 From enhanced diffusion to ultrafast ballistic motion of hybrid light–matter excitations *Nat. Mater.* **22** 338–44
[153] Jin L, Sample A D, Sun D, Gao Y, Deng S, Li R, Dou L, Odom T W and Huang L 2023 Enhanced two-dimensional exciton propagation via strong light–matter coupling with surface lattice plasmons *ACS Photonics* **10** 1983–91
[154] Sokolovskii I, Tichauer R H, Morozov D, Feist J and Groenhof G 2023 Multi-scale molecular dynamics simulations of enhanced energy transfer in organic molecules under strong coupling *Nat. Commun.* **14** 6613
[155] Dang N H M, Zanotti S, Drouard E, Chevalier C, Trippé-Allard G, Deleporte E, Seassal C, Gerace D and Nguyen H S 2024 Long-range ballistic propagation of 80% excitonic fraction polaritons in a perovskite metasurface at room temperature *Nano Lett.* **24** 11839–46
[156] Tichauer R H, Sokolovskii I and Groenhof G 2023 Tuning the coherent propagation of organic exciton-polaritons through the cavity Q-factor *Adv. Sci.* **10** 2302650
[157] Chen Y, Shi Y, Gan Y, Liu H, Li T, Ghosh S and Xiong Q 2023 Unraveling the ultrafast coherent dynamics of exciton polariton propagation at room temperature *Nano Lett.* **23** 8704–11
[158] Zakharko Y, Rother M, Graf A, Hähnlein B, Brohmann M, Pezoldt J and Zaumseil J 2018 Radiative pumping and propagation of plexcitons in diffractive plasmonic crystals *Nano Lett.* **18** 4927–33
[159] Yadav R K, Otten M, Wang W, Cortes C L, Gosztola D J, Wiederrecht G P, Gray S K, Odom T W and Basu J K 2020 Strongly coupled exciton–surface lattice resonances engineer long-range energy propagation *Nano Lett.* **20** 5043–9
[160] Pandya R *et al* 2021 Microcavity-like exciton-polaritons can be the primary photoexcitation in bare organic semiconductors *Nat. Commun.* **12** 6519
[161] Liu B, Lynch J, Zhao H, Conran B R, McAleese C, Jariwala D and Forrest S R 2023 Long-range propagation of exciton-polaritons in large-area 2D semiconductor monolayers *ACS Nano* **17** 14442–8
[162] Deveaud B 2015 Exciton-polariton Bose-Einstein condensates *Annu. Rev. Condens. Matter Phys.* **6** 155–75
[163] Griffin A, Snoke D W and Stringari S 1996 *Bose-Einstein Condensation* (Cambridge University Press)
[164] Hakala T K, Moilanen A J, Väkeväinen A I, Guo R, Martikainen J-P, Daskalakis K S, Rekola H T, Julku A and Törmä P 2018 Bose–Einstein condensation in a plasmonic lattice *Nat. Phys.* **14** 739–44
[165] Sun Y, Wen P, Yoon Y, Liu G, Steger M, Pfeiffer L N, West K, Snoke D W and Nelson K A 2017 Bose-Einstein condensation of long-lifetime polaritons in thermal equilibrium *Phys. Rev. Lett.* **118** 016602
[166] Alnatah H, Yao Q, Beaumariage J, Mukherjee S, Tam M C, Wasilewski Z, West K, Baldwin K, Pfeiffer L N and Snoke D W 2024 Coherence measurements of polaritons in thermal equilibrium reveal a power law for two-dimensional condensates *Sci. Adv.* **10** eadk6960
[167] Fontaine Q *et al* 2022 Kardar–Parisi–Zhang universality in a one-dimensional polariton condensate *Nature* **608** 687–91
[168] Plumhof J D, Stöferle T, Mai L, Scherf U and Mahrt R F 2014 Room-temperature Bose–Einstein condensation of cavity exciton–polaritons in a polymer *Nat. Mater.* **13** 247–52
[169] Dusel M, Betzold S, Egorov O A, Klembt S, Ohmer J, Fischer U, Höfling S and Schneider C 2020 Room temperature organic exciton–polariton condensate in a lattice *Nat. Commun.* **11** 2863
[170] Kéna-Cohen S and Forrest S R 2010 Room-temperature polariton lasing in an organic single-crystal microcavity *Nat. Photon.* **4** 371–5
[171] Su R, Diederichs C, Wang J, Liew T C H, Zhao J, Liu S, Xu W, Chen Z and Xiong Q 2017 Room-temperature polariton lasing in all-inorganic perovskite nanoplatelets *Nano Lett.* **17** 3982–8
[172] De Giorgi M, Ramezani M, Todisco F, Halpin A, Caputo D, Fieramosca A, Gomez-Rivas J and Sanvitto D 2018 Interaction and coherence of a plasmon–exciton polariton condensate *ACS Photonics* **5** 3666–72
[173] Zhang L, Hu J, Wu J, Su R, Chen Z, Xiong Q and Deng H 2022 Recent developments on polariton lasers *Prog. Quantum Electron.* **83** 100399
[174] Yagafarov T *et al* 2020 Mechanisms of blueshifts in organic polariton condensates *Commun. Phys.* **3** 1–10
[175] Lagoudakis K G, Wouters M, Richard M, Baas A, Carusotto I, André R, Dang L S and Deveaud-Plédran B 2008 Quantized vortices in an exciton–polariton condensate *Nat. Phys.* **4** 706–10
[176] Liew T C H, Kavokin A V, Ostatnický T, Kaliteevski M, Shelykh I A and Abram R A 2010 Exciton-polariton integrated circuits *Phys. Rev.* B **82** 033302
[177] Liew T C H, Kavokin A V and Shelykh I A 2008 Optical circuits based on polariton neurons in semiconductor microcavities *Phys. Rev. Lett.* **101** 016402
[178] Moxley F I, Ilo-Okeke E O, Mudaliar S and Byrnes T 2021 Quantum technology applications of exciton-polariton condensates *Emerg. Mater.* **4** 971–88
[179] Feng J, Li H, Sun Z and Byrnes T 2023 Entanglement generation and detection in split exciton-polariton condensates *Phys. Rev.* A **108** 053301